MDPI

Article

Investigation of the Geological Structure of the Tramutola Area (Agri Valley): Inferences for the Presence of Geofluids at Shallow Crustal Levels

Fabio Olita [1,*], Valeria Giampaolo [2], Enzo Rizzo [2,3], Giuseppe Palladino [4], Luigi Capozzoli [2], Gregory De Martino [2] and Giacomo Prosser [1]

1   Department of Science, University of Basilicata, 85100 Potenza, Italy
2   Institute of Methodologies for Environmental Analysis, National Research Council, C. da S. Loja, 85050 Potenza, Italy
3   Department of Physics and Earth Sciences, University of Ferrara, 44121 Ferrara, Italy
4   Department of Geology and Geophysics, School of Geosciences, University of Aberdeen, Aberdeen AB24 3FX, UK
*   Correspondence: fabio.olita@unibas.it

Abstract: The Tramutola area in the High Agri Valley represents a key for the Southern Apennines fold and thrust belt. There, natural oil seeps from small carbonate reservoirs located at shallow depths that have been historically known since the 19th century, and hypothermal water was discovered during hydrocarbon exploration. From a geological point of view, the study area, extending for about 11 km^2, is characterized with the presence of a complete section of the tectonic units of the southern Apennines and a complex structural framework that has not yet been fully clarified. In this work, geological analysis is based on new lithological and structural data, acquired during a detailed geological survey, compared with well logs obtained during exploration for hydrocarbons. Furthermore, a new geophysical investigation down to a 1 km depth (deep electrical resistivity tomography) allowed inference of buried structural and geological characteristics of the studied area. Through combining surface and subsurface data, some preliminary considerations about the structural setting and geofluid presence down to a 1 km depth have been made. Furthermore, geological–structural cross-sections have been constructed with the purpose of depicting the geometries of structures affecting the Apennine nappe pile in the subsurface, possibly favoring early uprising of hydrocarbons as well as circulation of hypothermal fluids and associated gases rising from deeper reservoirs.

Keywords: field geology; structural analysis; deep geophysics; Southern Apennines; digital processing; geofluid reservoir

1. Introduction

One of the goals enshrined in the United Nations 2030 Agenda is to ensure access to affordable, safe, sustainable and modern energy for all and to contribute to addressing climate change and its impacts. An effective solution is represented with using geothermal energy, a natural resource characterized with low greenhouse-gas emissions and a small environmental footprint [1]. Furthermore, repurposing of onshore hydrocarbon wells for production and/or storage of geothermal heat has recently been considered as a valuable opportunity for decarbonization of the heat and energy supplies worldwide [2,3].

Although efforts to repurpose abandoned onshore hydrocarbon wells into geothermal resources have increased in the last decade, many social, technical, economic and regulatory issues still remain to be solved. Furthermore, availability and quality of data on geothermal reservoirs and resources and the wells' characteristics (lithologies, designs and states of cementation) represent a challenge for many old oil and gas fields [4]. Therefore, repurposing old onshore hydrocarbon wells into geothermal ones requires a deep review

of old data; new, detailed geological- and geophysical-data acquisition; and integration of surface and subsurface datasets. This multidisciplinary approach has proved to be a powerful tool in unraveling subsurface geological and structural complexity and providing useful suggestions for reconstructing deep and shallow fluid circulation in geothermal applications [5,6].

In this paper, the integration of old and new geological and geophysical data is proposed to preliminarily characterize geothermal reservoirs and assess geothermal resources in an abandoned hydrocarbon reservoir in Italy. This multidisciplinary approach was tested in the High Agri Valley oil field, Europe's largest onshore hydrocarbon reservoir (Basilicata region). In this area, hydrocarbon exploration began in the early 20th century as a result of interest in natural hydrocarbon springs, within the Tramutola village (Basilicata), which were already known thanks to oral testimonies at the end of the 19th century [7]. These natural oil spills testified to the presence of hydrocarbons in the subsurface, which, due to the peculiar historical period and increasing scientific and technological knowledge, was beginning to be of economic and political interest for energy reasons [7].

The first studies were performed by Camillo Crema [8] and Guido Bonarelli [9], who contributed to the first interpretation of the geology of the area and to the drafting of the first geological maps. Hydrocarbon exploration was started in 1936 by public bodies and private companies; in detail, the Tramutola oil field consisted of 48 wells, mostly unproductive, that generally reached depths of a few hundred meters. Only the TRA_45 well, drilled during the years1958–1959, reached the depth of 2000 m. Generally, well logs reported small quantities of oil and gas in different formations [7,10]. Consequently, because of its low economic value, the Tramutola permit was abandoned in 1959 and officially closed in 1970 [11]. Hydrocarbons are not the only fluids of interest in the area. In fact, during the drilling of the TRA_2 well (1936, 404.4 m), a considerable amount of sulphureous hypothermal water (~28 °C with a flow rate of 10 L/s) with associated gases (mainly CH_4 and CO_2) was discovered.

Despite past economic interest, few studies concerning the geological setting of the Tramutola area have been published so far. Geological data and some reports on industrial activities carried out between the 1940s and 1960s are available in the ViDEPI project (www.videpi.com, accessed on 10 January 2022) [12,13]. On this free database, the TRA_45 well log and two low-quality seismic profiles (lines PZ-350-79 and PZ-5), acquired in 1976 and 1979, respectively, are available. They cross the Agri Valley and pass, respectively, within and immediately south of the study area.

The Tramutola area falls in the vicinity of the Agri Valley oil field, which has been of interest for large-scale deep geophysical prospecting, i.e., reflection seismic and magnetotelluric (MT) investigations carried out for exploration of the oil field hosted in the carbonates of the Apulian Platform and characterization of deep structures in the Southern Apennine fold and thrust belt [14–22]. In particular, an isobath map of the top Apulian carbonates has been reconstructed by Nicolai and Gambini [23], whereas MT data published by Balasco et al. [21,22] shed light on deeper crustal levels. Through integration of surface and subsurface geological and geophysical data, crustal sections through the Southern Apennines, crossing the Agri Valley oil field at about 6 km south of the study area, have been constructed by several authors [14,15,24–26]. Furthermore, some remarks have been made about the geothermal potential of the same area [20,27]. Despite their valuable contribution to crustal studies, these cross-sections are generally characterized with poor resolution in the shallower portion of the crust. Finally, the seismicity of the Agri Valley area has been studied by several authors [28–33], while the correlation between local seismicity and the hydrogeological and geochemical signals of the hypothermal water and gas upwellings from the TRA_2 well has been analyzed by Cello et al. [34], Italiano et al. [35] and Colangelo et al. [36].

In the last years, the use of deep electrical resistivity tomography (DERT) has become more common for investigation of areas with complex geological settings. The considerable resolution obtained through such a technique, compared to MT surveys, makes it possible to

much more effectively discriminate resistivity contrasts existing in the shallower subsurface, thus providing more reliable information on physical conditions of rocks and the presence of fault surfaces as well as of aquifers and/or fluids of various origins [37–47]. In the past years, several DERT applications to a 1 km depth have been carried out exclusively to characterize the High Agri Valley sedimentary basin [48,49], but they have never been carried out in the study area.

This work proposes the integration of old well data and new geological, structural and geophysical data in order to preliminarily infer geofluid presence and circulation in the Tramutola area through the combination of the surface and subsurface data derived from wells and DERT interpretation. During the evolution of the Southern Apennines fold and thrust belt, the development of differently oriented low- to high-angle fault sets shaped the structural complexity of the studied area. This tectonic setting influences underground geofluid circulation, which is not easy to interpret. The study of the geological and structural setting of the Tramutola area is therefore important in order to better understand how tectonic structures may affect distribution and migration of geofluids. In addition, detailed field and subsurface data might be used to shed light on the emplacement mechanisms of allochthonous units in the southern Apennines fold and thrust belt.

2. Geological Setting

2.1. Southern Apennines

The Apennine chain is an Oligocene-to-Pliocene, NW-trending orogen resulting from the collision between the African and Eurasian lithospheric plates ([14,15,50–52] and references therein). The southern sector of the chain is a NE-vergent fold and thrust belt, formed between the Miocene and Pleistocene periods, mostly consisting of sedimentary successions, with minor igneous and metamorphic rocks [53]. It represents the northern sector of the Apennines–Maghrebide chain that continues southward in the NE-trending Calabrian domain and in the nearly E-trending Sicilian Maghrebides. The arcuate shape of the orogen has been produced through the progressive retreat of the Ionian subduction toward the SE, which was also responsible for the formation of the Tyrrhenian Sea in a back-arc position [54–57]. The migration of the Calabrian domain toward the SE and the simultaneous opening of the Tyrrhenian back-arc basin from the upper Miocene period have conditioned the tectonic evolution of the whole Apennine Chain [58].

The Southern Apennine Chain is composed of allochthonous tectonic units consisting of sedimentary cover successions detached from the original basement (Figure 1). These tectonostratigraphic units, corresponding to specific paleogeographic domains [52], are arranged from west to east as (i) the Liguride and Sicilide Complexes, (ii) the Apennine Platform Units, (iii) the Lagonegro Basin Units and (iv) a frontal imbricate fan. All these units overlie the (v) Jurassic–Cretaceous limestone of the Apulian Platform covered with (vi) Eocene and Miocene breccia, with calcarenite and evaporite, and with the (vii) Pliocene–Pleistocene terrigenous successions of the Bradanic foredeep [59].

The tectonic evolution of the southern Apennines is characterized with phases of contractional deformation developed from the Miocene to the Pliocene period, producing superposition of different tectonic units, followed by extensional processes developed from the Pliocene to the Quaternary period. During the contractional phase, development of major thrust surfaces allowed staking of the different tectonic units with a NE vergence. After the contractional phase, since the Late Pliocene period, the tectonic edifice was affected by low-angle normal faults (LANFs), which partly resulted from inversion of the previous thrust surfaces [25,60]. During the Quaternary period, both contractional structures and low-angle normal faults were affected by high-angle transtensional and normal faults (HANFs), with consequent opening of intermontane basins, such as the Agri Valley [25,60,61].
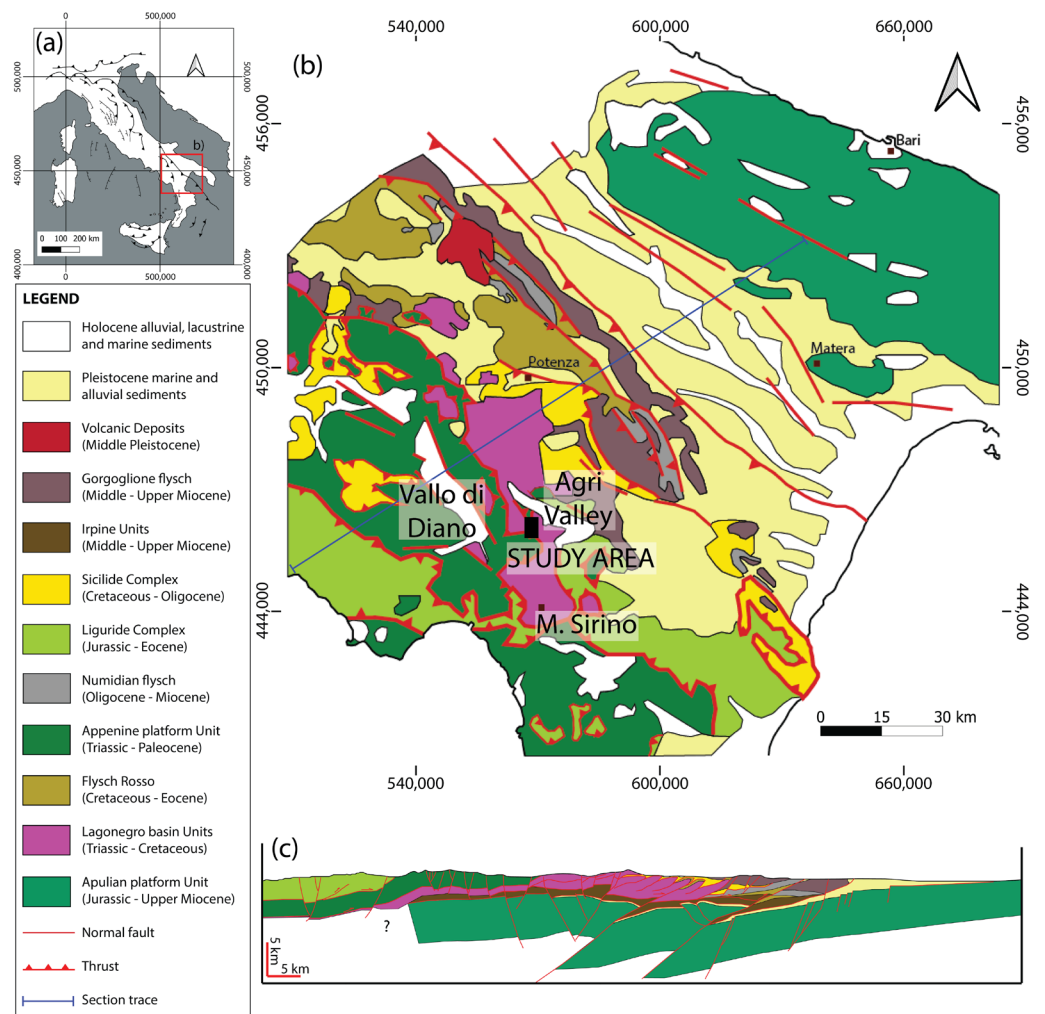
Figure 1. (**a**) Structural map of Italy and legend of the geological map and cross section; (**b**) Geological–structural map of the Southern Apennines. (**c**) Regional geological cross-section across the Southern Apennines from the SW to the NE, redrawn and modified based on Piedilato and Prosser [62].

2.2. Geology of the High Agri Valley

The studied area falls within the Cavolo valley, located along the southwestern side of the High Agri Valley and bounded to the west with the carbonate ridge of Monti della Maddalena (Figure 2).

The Agri Valley is a NW–SE-trending tectonic depression filled with Quaternary continental deposits, located in the axial sector of the Southern Apennines (Figure 2) and bounded with transtensional to extensional faults [61].

The valley flanks expose a series of tectonic units consisting of Mesozoic and Cenozoic sedimentary rocks, represented from top to bottom with the Sicilide and the Liguride Complexes, the Apennine Platform and the Lagonegro Units [60]. The Liguride Complex consists of Cretaceous and Cenozoic flysch resting along a low-angle tectonic contact on the Apennine Platform or the Lagonegro Units (Figure 2). Generally, in the southern sector of the Agri valley, the base of the Liguride Complex is represented with the Crete Nere and Saraceno Formations [63]. In the study area, the basal interval is represented with the Cavolo Formation, consisting of alternating calciclastic and siliciclastic turbidites and black shale, of late Eocene–Oligocene period [63] or to the Cretaceous–Paleocene period [64–66]. The topmost stratigraphic unit of the Liguride Complex is represented with the Albidona Formation, widely exposed along both sides of the Agri Valley. It consists of a more than 1 km-thick succession of clay, turbiditic sandstones and microconglomerate, with some typical marly intervals that are particularly frequent in the lower part of the succession [67].

The Liguride Complex rests tectonically on the Apennine Platform Units, mostly consisting of the Monti della Maddalena Unit, which is interpreted as being derived from the eastern margin of the Apennine carbonate platform [68,69]. The platform carbonates consist of Late Triassic–Early Jurassic basal dolomite and dolomitic limestone, followed upward by laterally discontinuous Late Jurassic to Early Cretaceous platform limestone, by talus breccias deposited from the Late Cretaceous to Eocene period and finally by terrigenous succession of the Bifurto Formation [69–71].

The Lagonegro Units represent the deeper tectonic-unit outcropping in the area and are covered with the Apennine Platform along a nearly horizontal thrust surface known as the Monti della Maddalena Thrust [28,60]. This structure is outlined with a pervasive cataclastic texture in upper Triassic dolomite. From bottom to top, the Lagonegro sequence consists of Early-to-Middle Triassic organogenic limestone, sandstone, siltstone and siliceous rocks of the Monte Facito Formation; upper Triassic cherty limestone of the Calcari con Selce Formation; Jurassic chert and shale of the Scisti Silicei Formation; and lower Cretaceous shale and marly limestone of the Galestri Formation [52]. The two major tectonic units derived from the Lagonegro Basin (Lagonegro I and II) display a similar stratigraphy, with more distal facies occurring in the Lagonegro I Unit [72,73]. In the High Agri Valley, the Lagonegro II Unit tectonically overlies the Lagonegro I Unit along the Marsico Nuovo thrust [57]. Pelagic rocks of the Lagonegro basin crop out mainly in the eastern sector of the High Agri Valley, where kilometer-scale anticlines allow the exposure of the deeper intervals of the Lagonegro I Unit. The age of thrusting of the Apennine Platform onto the Lagonegro Units and of the Lagonegro II Unit onto the Lagonegro I Unit is indicated with the syntectonic deposition of the Langhian to Tortonian Gorgoglione Formations [52].

Folds exposed on the western and eastern sides of the Agri Valley display different orientations. More specifically, the Monte Sirino area (Figure 1) and the northeastern sector of the Agri Valley show different vergences and orientations for thrusts and folds. The shortening recorded for the large thrust fault in the northern area of Monte Sirino [25] shows kinematic indicators consistent with an NNE-directed tectonic transport. This deformation is related to the first phase of thrusting activity. On the contrary, the Marsico Nuovo and Monte Enoc–Caldarosa areas (Figure 2) display km-scale anticline folds mainly characterized with N–S-trending axes [51].

In the subsurface of the Agri Valley, the Lagonegro Units rest tectonically on a sequence of Mesozoic to Tertiary carbonates of the buried Apulian Platform, covered with Early Pliocene siliciclastic rocks [18]. The tectonic contact between the Early Pliocene siliciclastic rocks and the overlying Lagonegro Units is outlined with a thick sequence of overpressurized Miocene siliciclastic sediments, interpreted as a tectonic mélange [18,74]. The buried Apulia carbonates underwent shortening during the Pliocene to Pleistocene periods, generating about 10 km-wide pop-up structures [15,75].

The subsequent Pleistocene evolution of the Agri Valley basin is connected to transtensional displacement along high-angle faults [61]. During the Early–Middle Pleistocene period, the Agri basin formed due to activity of left-lateral N120°-trending transtensional faults, whereas N-trending faults were located mainly along the western border of the basin. Further subsidence and widening of the basin during the Middle Pleistocene period were connected to reactivated or newly formed NW-trending normal faults [76]. Presently, two major fault systems with different average orientations bound the tectonic depression of the Agri Valley; on the western side, the Monti della Maddalena Fault System (MMFS) is mostly represented with NW–SE faults, while on the eastern side, the Eastern Agri Fault System (EAFS) mostly consists of N120°-trending faults [28,30]. Recently, Brozzetti [77] highlighted a regional array of normal faults, in the southern Apennines of Italy, that were active during the Quaternary period and are referred to as the "Campania-Lucania Extensional Fault System" (CLEFS), consisting of three main NW–SE-striking alignments of low-angle normal faults.
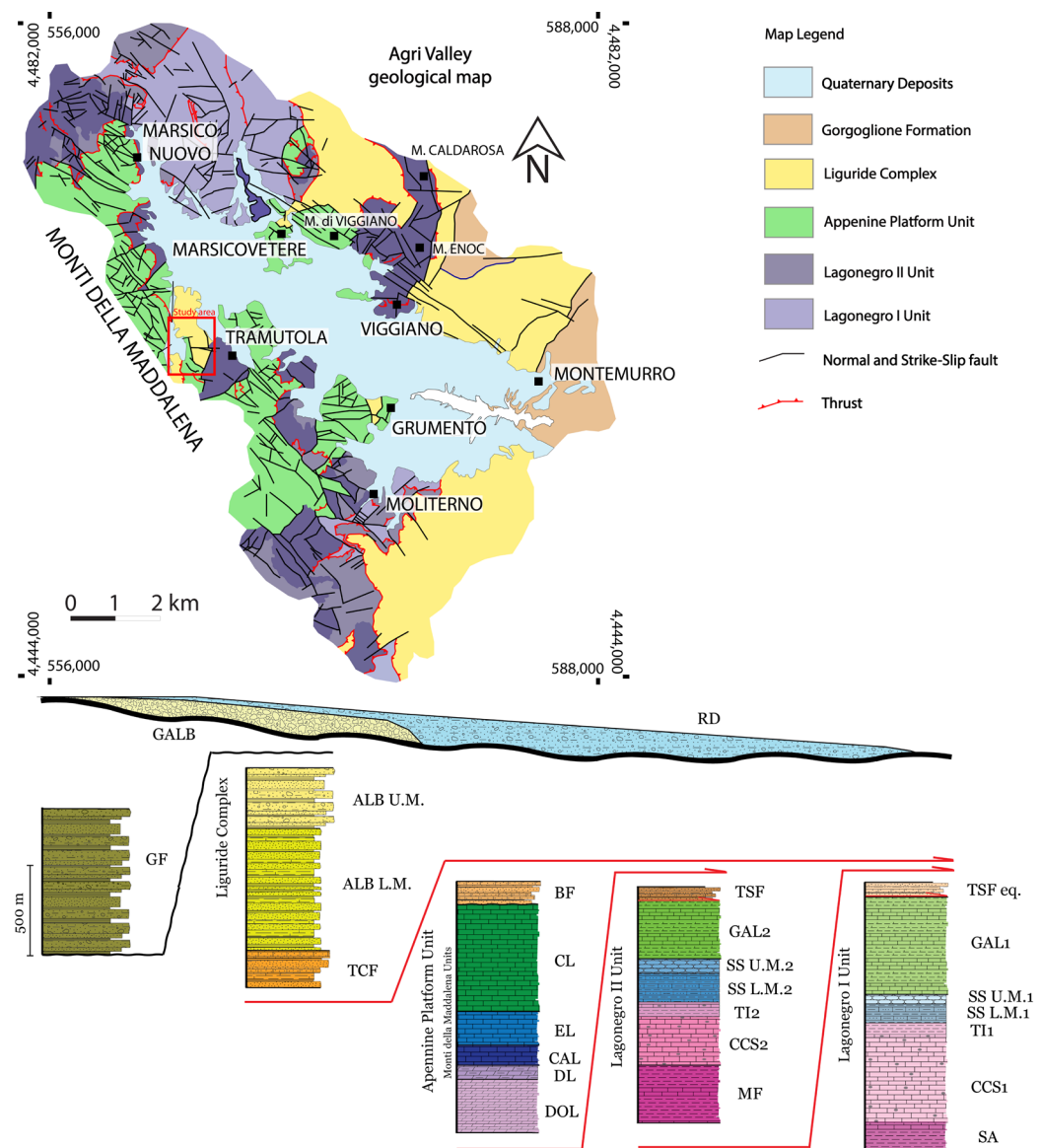
Figure 2. Geological–structural map of the Agri Valley modified from published geological maps [78–82]; the red box identifies the study area. Stratigraphic–structural scheme of the tectonic units exposed in the Agri Valley. Recent deposit (RD), Galaino breccia (GALB), Gorgoglione Formation (GF), Albidona Formation upper member (ALB U.M.), Albidona Formation lower member (ALB L.M.), Torrente Cavolo Formation (TCF), Bifurto Formation (BF), crystalline limestone (CL), Ellipsactinia limestone (EL), calcirudite (CAL), dolomitic limestone (DL); for Lagonegro II Unit: Torrente Serrapotamo Formation (TSF), Galestri Formation (GAL2), Scisti Silicei upper member (SS U.M.2), Scisti Silicei lower member (SS L.M.2), transitional interval (TI2), Calcari Son Selce Formation (CCS2), Monte Facito Formation (MF); for Lagonegro II Unit: Torrente Serrapotamo equivalent Formation (TSF eq.), Galestri Formation (GAL1), Scisti Silicei upper member (SS U.M.1), Scisti Silicei lower member (SS L.M.1), transitional interval (TI1), Calcari Son Selce Formation (CCS1), Sorgente Acero Formation (SA).

3. Data and Methods

This area has been studied through means of a multimethod approach, including geological field mapping, scouting for geolocalization of well heads associated with extraction activity in the years 1936–1959, analysis of well logs and realization and interpretation of deep electrical resistivity tomography (DERT) longitudinal to the Cavolo stream valley and passing in proximity of the TRA_2 well (Figure 3).
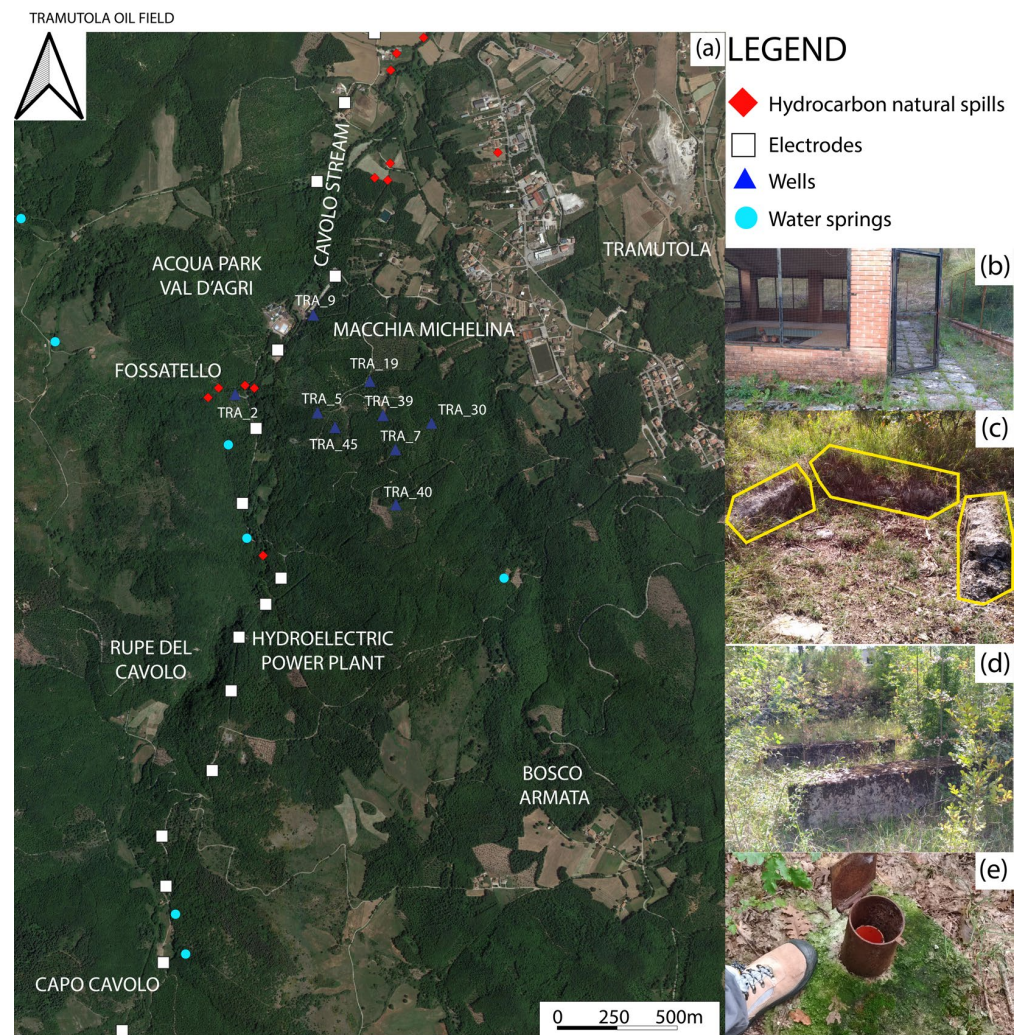
Figure 3. (**a**) Locations of natural oil spills, electrodes used for the DERT, wells of the Tramutola oil field and water springs on a Google Earth image; (**b**) the TRA_ 2 well; (**c**,**d**) concrete blocks (highlighted with yellow box in (**c**)) of the extraction plant; and (**e**) the wellhead.

3.1. Field Analysis

Geological mapping was carried out in an area extending for about 11 km^2 (Figure 3), which includes all the wells drilled during exploitation of the Tramutola oil field. We used as a starting point for the field work the 1:50,000 geological map of the Agri Valley by Carbone et al. [78] and the following sheets of the geological map of Italy: sheet 210 "Lauria" [79] at the 1:100,000 scale and sheets 489 "Marsico Nuovo", 505 "Moliterno" and 506 Sant'Arcangelo [80–82] at the 1:50,000 scale. Due to the intense vegetation occurring in the study area, field analysis was preceded with a detailed search of all the outcrops on a high-resolution DTM and satellite images on Google Earth. The identified outcrops were described from a geolithological point of view and associated with the geological units documented in the scientific literature. Bedding planes, low- and high-angle fault planes and fold axes were measured with the means of a geological compass. Outcrops and geological structures were geolocated through the Geopaparazzi open-source app for Android phones, by HydroloGIS S.r.l. (http://www.geopaparazzi.org, accessed on 10 January 2022). Georeferenced data were processed with the means of open-source QGIS software (https://www.qgis.org, accessed on 10 January 2022), using the digital topography, at a 1:5000 scale, of the Basilicata region (RSDI Basilicata; https://rsdi.regione.basilicata.it, accessed on 10 January 2022) to obtain a geological–structural map.

3.2. Well Scouting and Analysis of Well Logs

The precise location of wells drilled from 1936 to 1959 in the study area was carefully verified through scouting in the field. The preparatory phase involved a preanalysis of high-resolution DTMs, satellite images from Google Earth and a study of topographic maps from the Eni archive. Scouting allowed identification of blocks, well heads and other tools used during exploration and exploitation of the Tramutola oil field. It should be noted that it was not possible to identify all 48 wells due to the lack of an updated bibliography regarding their precise location and because of the long time that has elapsed since the last well was drilled (1959 for the Tra_45 well). Natural hydrocarbon spills were also identified, mapped and compared with the pioneering study by Bonarelli [83]. The identified handworks and oil spills were geolocated and reported in the QGIS software. By these means, 22 well heads and 13 oil spills were identified and precisely located on a 1:5000 topographic map (Figure 3).

Finally, well logs were analyzed to identify top formations and mineralized levels. The stratigraphy of the well logs was compared with the formations exposed in the High Agri Valley. The location of the TRA_45 well was deduced from the data reported in the composite well log, available in the ViDEPI project (www.videpi.com, accessed on 10 January 2022).

3.3. Deep Electrical Resistivity Investigation

The direct-current (DC) electrical resistivity method consists of experimental determination of the apparent resistivity parameter (ρ_a, Ωm) through joint measurements of electric-current intensity (I, Ampere), sent into the subsoil through the means of a pair of electrodes (A and B) embedded in the ground, and voltage (ΔV, volt) at the ends of a second pair of electrodes (M and N), also in direct contact with the ground (Figure 4a). The apparent resistivity values are obtained from the following relationship:

$$\rho_a = K \frac{V}{I} \tag{1}$$

where K (m) is the geometric coefficient depending on the arrangement of electrodes on the ground surface. As the positions of the injected (AB) and acquired (MN) pairs of electrodes are moved in the investigated area, a tomographic image of the subsoil electrical resistivity is produced. This is called electrical resistivity tomography (ERT). For each arrangement of electrodes, an apparent electrical resistivity value is obtained. This is the resistivity obtained, assuming that the volume of the material being measured is completely homogenous. To move from apparent resistivity to "true" resistivity, inversion software is used. The principle of inversion software consists of an inversion routine implemented through an optimization technique to calculate a two-dimensional resistivity model for the subsurface from data acquired at the surface using various electrode combinations. The optimization method modifies the resistivity model through iteratively reducing the difference between the measured apparent resistivity values and those calculated with the model.

In relatively shallow investigation (e.g., x < 300 m), ERTs are carried out using multi-channel systems able to provide a large number of measurements in a short time. However, multichannel systems are characterized with poor depth of investigation due to the need for a single cable to connect the electrodes with the control system. In order to obtain information at greater depths, it is necessary to use a "decoupled" measuring system, i.e., one with a separate transmitter and receiver. This configuration, identified as deep electrical resistivity tomography (DERT), allows us to reach investigation depths spanning between 400 m and more than 1 km [84]. At the same time, the characteristics of the transmitting system impose favorable logistical conditions that allow the energizer and generator to be easily moved and cables to be laid up for to 1 km.
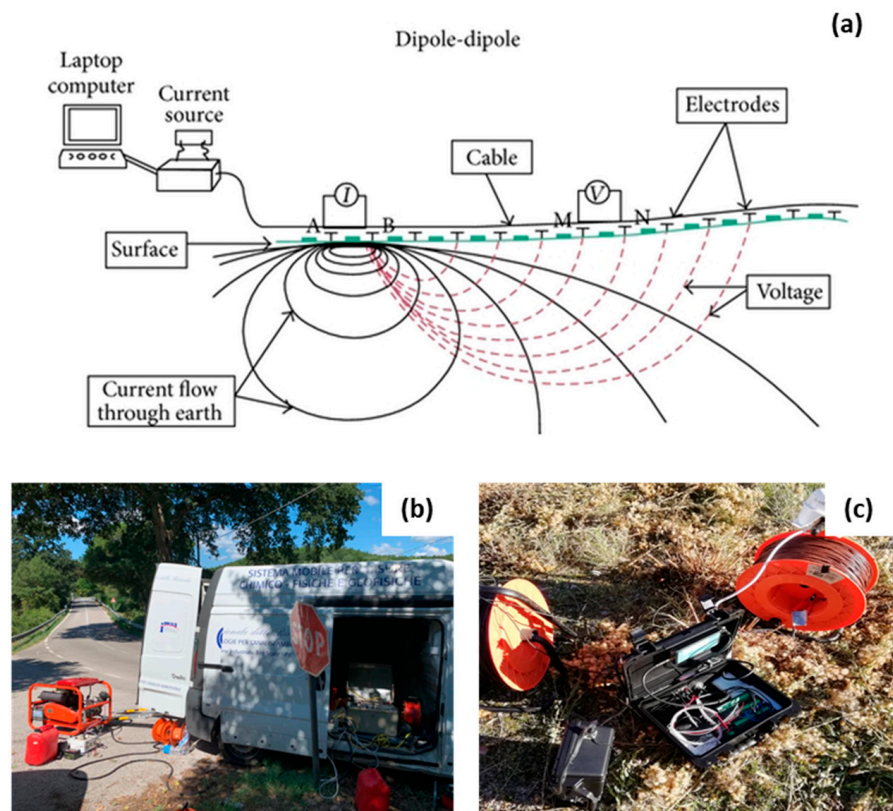
Figure 4. (**a**) Principles of the shallow DC electrical resistivity survey [85]. (**b**) DERT energizing system and (**c**) DERT measuring system.

Focusing on the Tramutola test area, the deep electrical resistivity survey lasted 3 days, of which the first day was dedicated to the installation of the first transmitting station and of 4 measuring stations along the profile to be investigated.

The transmitting system consisted of 1 m-long stainless-steel current electrodes (AB) connected via log monopolar cables to the GGT-10 transmitter and the ZMG-9 power system (Zonge Ltd., Tucson, AZ, USA, Figure 4b). The measuring system consisted of standard stainless-steel potential electrodes (MN) connected via log monopolar cables to a datalogger, radio-connected to a personal computer and capable of recording a total number of 8 potential differences (mV) each second (Figure 4c). Both the energizing and measuring systems were equipped with a GPS antenna recording position and timing each second. This last information is useful for synchronization of current and electrical potential data.

For each current dipole (AB), a square wave of 32 s was injected into the subsoil for 15–20 min, and current and electric potential signals (at MN) were simultaneously acquired, with a sampling rate of 1 s. A maximum energizing current of 9 A was injected into the ground (2–9 A).

The DERT at the Tramutola site was acquired using 17 electrodes with distances varying between 250 and 350 m (locations are shown in Figure 3). In this way, the total length of the profile was approximately 4800 m. The current and potential electrodes were arranged with dipole–dipole (DD) electrode configuration using dipole lengths spanning from 250 to 1100 m. In this way, it was possible to reach an investigation depth of about 1000 m. In total, 4 energizing stations and 18 current dipoles were used; moreover, 195 electric potential datasets were measured.

4. Results

4.1. Stratigraphic and Structural Setting of the Study Area

4.1.1. Stratigraphic Setting of the Tramutola Area

Results of the detailed geological field analysis indicate that some significant intervals of the stratigraphic successions belonging to the Liguride Complex, the Apennine Platform and the Lagonegro Units are exposed in the study area. This is illustrated in the detailed geological map, at a 1:5000 scale, realized from the field survey (Figure 5).
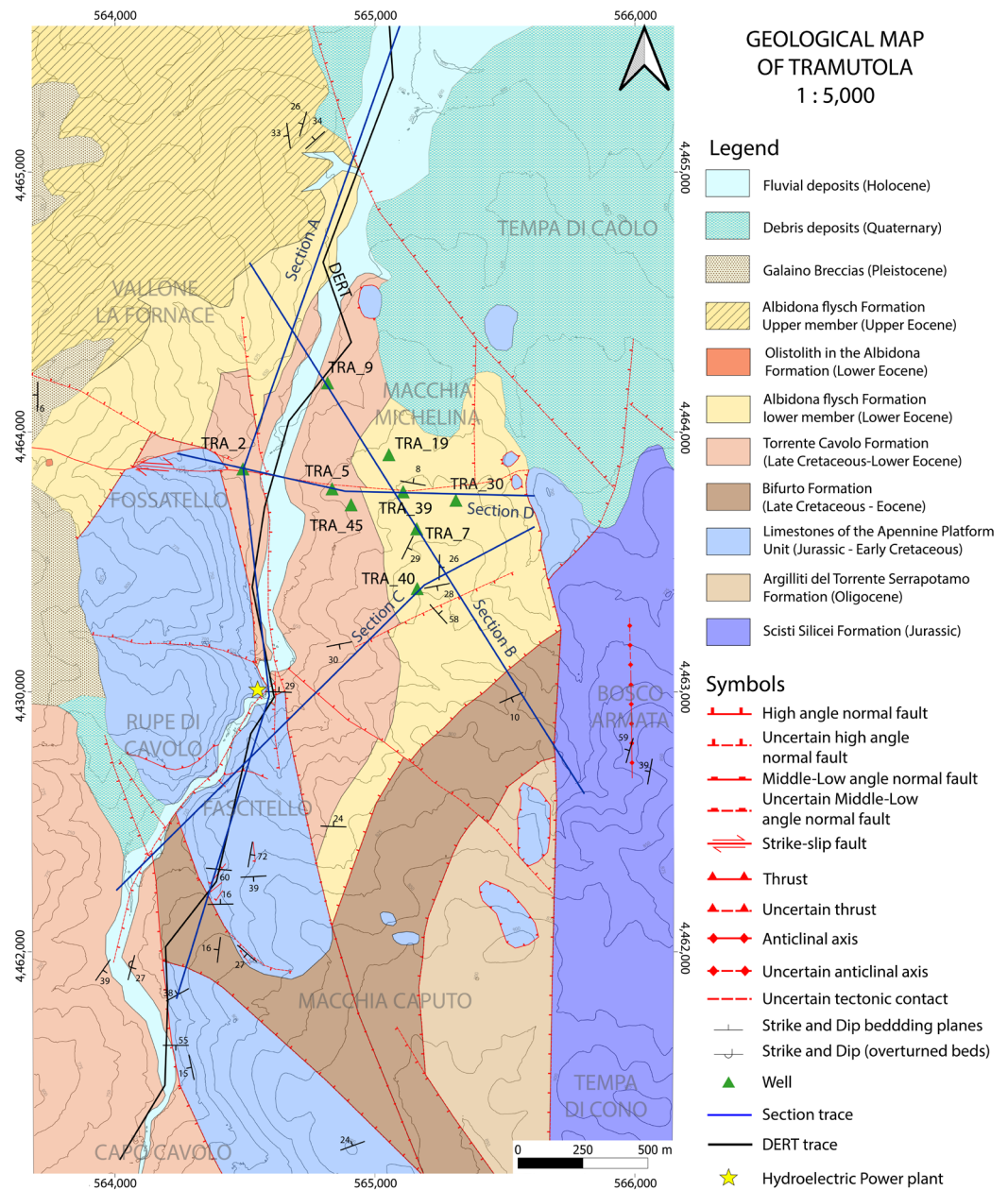

Figure 5. Geological map of the study area.

The lower part of the Liguride Complex is represented with a Late Cretaceous–Eocene succession consisting of the calciclastic turbidites of the Torrente Cavolo Formation [65], while the upper part is represented with alternating clays, marls, arenaceous turbidites and coarse-grained sandstone and conglomerates(Albidona Formation).

The Torrente Cavolo Formation is exposed in small outcrops along the Cavolo stream in the central sector of the study area. There, the Formation consists of 10–20 cm-thick beds of laminated, mainly calciclastic arenites containing rare chert nodules and occurring within black shale and marls. Intense deformation, together with poor outcrop conditions, prevented a detailed stratigraphic reconstruction of the Torrente Cavolo Formation. The contact with the overlying Albidona Formation is marked with massive marls and cal-cilutites in about 10 m-thick bed packages, outcropped in the Vallone La Fornace Gorge (Figure 5). Exposures of the Albidona Formation are mainly present along the western side of the Cavolo valley (Figure 5). There, the Formation can be divided into two members, following in part the subdivision proposed by Baruffini et al. [68] for type locality. The lower member is characterized with the presence of about 10 m-thick strata of marls and calcilutites, occurring within dominant gray clay and subordinate sandstone strata. A mass transport deposit containing metric sized blocks of pink granite and mafic rocks is present on top of the uppermost marly horizon. This olistostrome layer, already described by previous authors, are placed in the Vallone La Fornace Gorge [86,87], and in other sectors of the Agri Valley [26,88]. The upper member mainly consists of alternating sandstone and microconglomerate and conglomerate beds and possibly corresponds to the D member described by Baruffini et al. [67] in the type locality.

The Apennine Platform Unit consists of dolostones, dolomitic limestone and limestone of the Late Triassic to Cretaceous age [64]. Due to intense brittle deformation, a complete stratigraphic succession is not present in the study area. Generally, carbonates of the Apennine Platform are in tectonic contact with the Liguride Complex or the Lagonegro Units, along low- and high-angle normal faults. The base of the succession, consisting of light gray Late Triassic dolostones, is exposed between the Tramutola Village and the Monti della Maddalena ridge. This unit is followed upward by dolomitic limestone, probably of the Jurassic age. In the study area (Figure 5), platform limestones are mostly exposed in an isolated block bordered with the Torrente Cavolo and Albidona Formations, located south of the TRA_2 well (Figure 5). There, limestone consists of calcilutites and oolitic, bioclastic or intraclastic calcarenites of the Toarcian to Late Jurassic age (according to ISPRA, the Moliterno Sheet of the Geological Map of Italy [82]), arranged in beds of 50 cm to some meters thick. In some cases, 30–40 cm-thick intervals of greenish marls separate the limestone layers. Interestingly, Late Triassic to Jurassic carbonates are locally characterized with the presence of hydrocarbons contained in tiny fractures.

The Lagonegro Unit is exposed in the southern and eastern sectors of the study area (Figure 5), where the only outcropping formation is represented with the Jurassic Scisti Silicei Formation, showing high-angle tectonic contacts with both the Liguride Complex and the Apennine Platform. The Scisti Silicei Formation of the Lagonegro II Unit (Figure 2), consists of reddish siliceous strata, with red shale and radiolarite levels occurring at the base. These well-bedded siliceous rocks are frequently affected by intense deformation, as indicated with the presence of fold trains in the Bosco Armata area (Figure 5). An almost complete succession of the Lagonegro II Unit, including the Calcari con Selce, Scisti Silicei and Galestri Formations, has been drilled in the Tra_45 well.

Finally, Pleistocene to Quaternary carbonate breccias, landslides and alluvial deposits cover part of the Meso-Cenozoic substrate in both the northeastern and the northwestern sectors of the study area.

4.1.2. Structural Setting

Evidence of contractional deformation can be documented in all the tectonic units exposed in the study area. In the Liguride Complex, this deformation is outlined with tight to isoclinal asymmetric folds, with a wavelength of some meters, particularly well-developed in the Torrente Cavolo Formation. These structures are well-exposed in the vicinity of the TRA_2 well and are characterized with N70°E-trending fold hinges. Similarly, the marly intervals of the Albidona Formation, exposed on the left side of the Cavolo Stream, are deformed by open folds with W-plunging hinges and a wavelength of about 100 m.

Folding also affects the Jurassic limestone of the Apennine Platform, as shown with a 10 m scale, as E- to SE-trending folds, with well-developed fracture cleavage in the hinge zone and steeply dipping limbs (Figure 6a). These structures are particularly well-developed along the left side of the Cavolo Stream, where a wide asymmetric anticline occurs at the hanging wall of a NE-dipping thrust (Figure 6b). Other minor ramp anticlines and duplex structures, showing NE-dipping striations consistent with a top-to-SW shear sense, can be observed in the Rupe di Cavolo area. In the Lagonegro Units, the Scisti Silicei Formation is intensely deformed by N-trending folds with chevron geometry and overturned limbs (Figure 6c).

The geological map in Figure 5 displays the major faults occurring in the study area. Some of the most important structures strike from N–S to NNW–SSE, such as the normal fault occurring along the Cavolo stream (Torrente Cavolo fault zone), nearly parallel to an NNW-striking medium- to low-angle normal fault exposed along the left side of the Cavolo stream between Fossatello and Rupe di Cavolo. Furthermore, in the southeastern sector of the study area, an N-striking, high-angle normal fault (Bosco Armata fault) separates the Scisti Silicei Formation in the footwall from the Serrapotamo and Bifurto Formations in the hanging wall. Minor E-striking, high-angle faults are present in the Macchia Michelina and Rupe di Cavolo areas, affecting the Liguride Complex and the Apennine Platform Units, respectively.

The NNW-striking medium- to low-angle normal fault is well-exposed northwest of the TRA_2 well, where it separates the Jurassic limestone at the footwall from the Torrente Cavolo Formation at the hanging wall. It displays an undulate slip surface with dip directions varying between N 50° and N 100°, and a nearly constant dip of 45°. Striations and slickenlines, marked with the preferred elongations of iron oxides on the slip surface, dip generally to the NE (between N 60° and N 70°), indicating nearly pure dip–slip kinematics (Figure 6d).

Southward, the same normal fault is exposed near the hydroelectric power plant located in the Cavolo Gorge (Figure 5), where a dip of 30° toward the NE was measured (Figure 6e). This structure terminates against the complex N-trending Torrente Cavolo fault zone, which separates the Jurassic limestone from the Liguride Complex. In this locality, the fault zone consists of two major fault strands separating a minor structural high formed of the Jurassic limestone in the southern part and the Torrente Cavolo Formation to the north. The two formations are separated with a NW-dipping low-angle normal fault characterized with a 10 m-thick damage zone in the Jurassic limestone of the footwall block. Other NW- and NE-striking normal faults, with minor strike-slip components, have been observed in the Jurassic limestone exposed in the Cavolo Gorge (Figure 6f). One of these faults offsets the NE-dipping thrust surface exposed at Rupe di Cavolo.

Another important N- to NNW-striking normal fault, separating the clayey lithologies of the Torrente Cavolo Formation in the hanging wall and the Jurassic limestone of the Apennine Platform in the footwall, is well-exposed in the southern sector of the study area. This fault is connected to the occurrence of the Capo Cavolo spring (Figure 5), with a flow rate of about 1000 liters per second [89].

The Fossatello fault is the most important E–W-striking structure in the study area. It is a strike-slip fault characterized with an about 10 m-wide fault zone, which is exposed into a deep gorge (Figure 6g). The fault core consists in an about 10 cm-thick fault breccia bounded with a N80°E striking-slip surface showing well-developed, nearly horizontal striations (striae 260/23, 260/10) and grooves indicating pure strike-slip kinematics (Figure 6h). Near the TRA_2 well, the Fossatello fault offsets the NW-trending, medium-angle normal fault with a dextral shear sense.
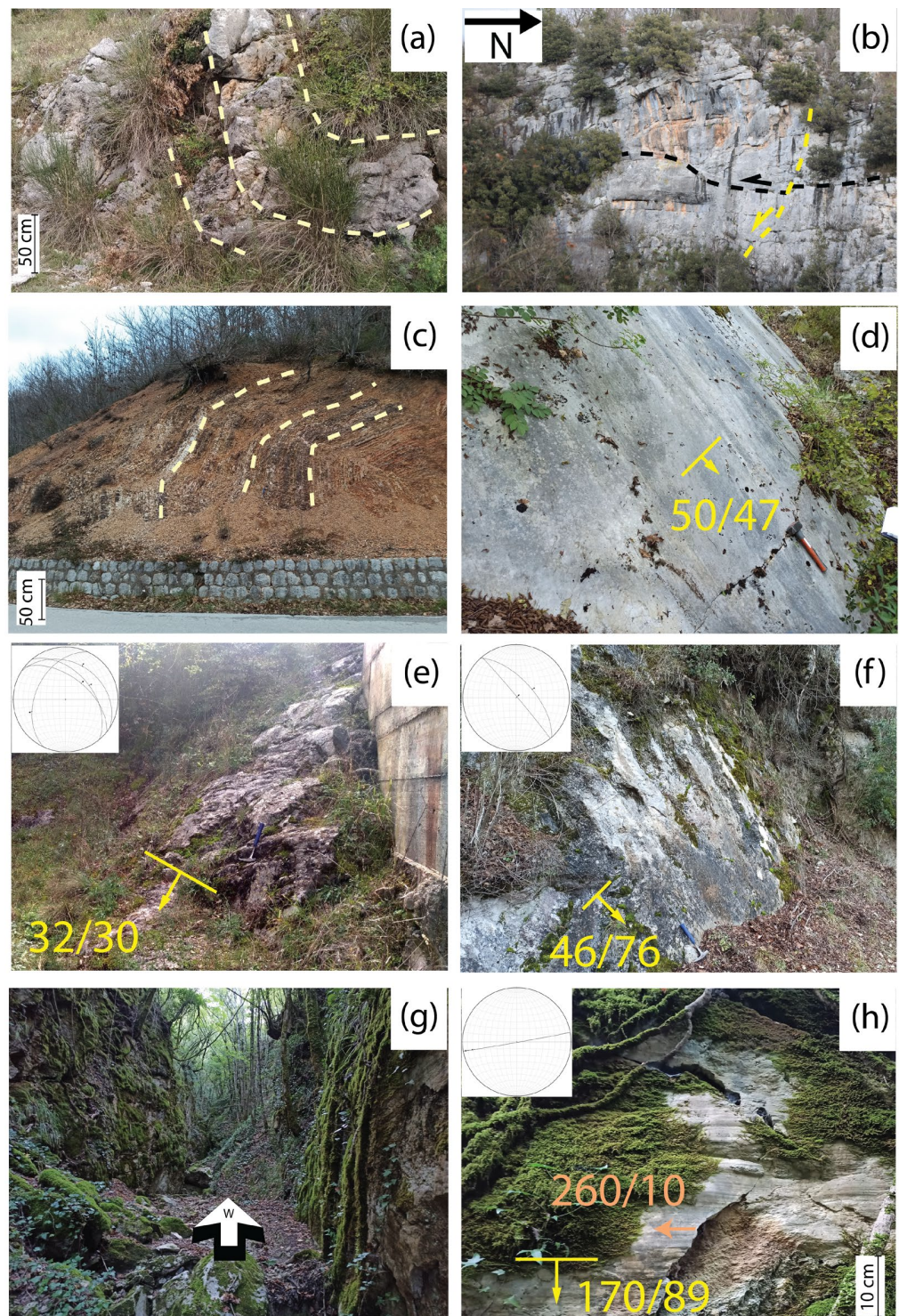
Figure 6. Examples of tectonic structures exposed in the study area: (**a**) folding affecting Jurassic limestone of the Apennine Platform, (**b**) thrust-related anticline in the carbonates of the Apennine Platform exposed along the left side of the Cavolo Gorge, (**c**) intense deformation in the Scisti Silicei

Formation (Lagonegro II Unit), (**d**) an example of a medium-angle normal fault near the Fossatello Gorge, (**e**) a low-angle normal fault near the hydroelectric power plant, (**f**) a NW-trending normal fault in the right side of the Cavolo Gorge and (**g**) the Fossatello right-lateral strike-slip fault in the Fossatello Gorge. (**h**) Detail of the Fossatello fault, showing horizontal striations and grooves. The stereonets in (**e**,**f**,**h**) represent the orientations of the striae and fault planes in the areas represented in the photographs.

The study of fracture porosity and permeability of the rock masses in the study area was limited by their scarce accessibility (Apennine Platform Unit) and the outcrop discontinuity (Lagonegro Units). In this respect, the pelagic carbonates of the Calcari con Selce Formation are relevant from a structural and hydrogeological point of view. This Formation is exposed outside of the study area, but it widely occurs in the subsurface. With previous authors taken into consideration [90–92], the succession is affected by folds and by high- and low-angle normal faults, which can potentially influence fluid circulation. Mazzoli and Di Bucci [90] and Mazzoli et al. [91] studied the development of faults from arrays of NE–SW-oriented en échelone veins in the Marsico Nuovo area (Figure 2). There, the average spacing of normal faults is 6.4 m. Novellino et al. [92] studied the brittle structures affecting the Calcari con Selce Formation of the Lagonegro II Unit outcropping near Potenza (Figure 1b). They highlighted the role of fractures in the damage zones of the LANFs in enhancing fluid circulation. Furthermore, the damage zones of the NE–SW-striking normal faults are highlighted with pervasive sets of fractures with considerable lengths.

4.2. Interpretation of the Subsurface in the Study Area
4.2.1. Well Data

Wells were drilled in the Macchia Michelina area (Figure 7a) and along the Cavolo Stream. According to the data reported in Figure S1, the maximum and minimum depths reached by the wells drilled in the period of 1936–1943 were 470.1 m (TRA_19 well) and 60 m (TRA_22 well), respectively.

The analysis of the well data was possible following several field inspections and with the aid of reference points obtained from the ViDEPI website. Once the geolocation of the wells had been verified, we proceeded with the analysis and interpretation of the well logs (P1000) provided by Eni. The P1000s (Figure S2) reported the results of percussion drilling up to depths of a few hundred meters. These descriptions allowed some formations and units to be identified accurately, such as the Scisti Silicei Formation and the Jurassic limestone of the Apennine Platform Unit (often described as whitish Mesozoic limestone). The other formations were hypothesized based on identification of reference intervals. The presence of dark gray clays and schistose marls identified the Torrente Cavolo Formation in the P1000s. Differently, the Albidona Formation is individuated in correspondence of marly layers and mica minerals in its description (Figure S3). Although it is often difficult to distinguish them, it is sometimes possible to differentiate these two formations based on the light and dark colors of the marly shale or on the abundance of calcite veins in the Torrente Cavolo Formation. Some difficulties have been encountered in differentiating the lithologies of the Torrente Serrapotamo and Galestri Formations. The former was often identified when dark, compact sandstones were present, while the latter was often characterized with gray and/or black laminated clays in the description. Finally, some intervals were interpreted based on their stratigraphic positions in the P1000s (Figure S1).

The upper interval reported in the P1000 of the TRA_45 well was reinterpreted considering its stratigraphic compatibility with the adjacent wells. The TRA_45 well, being the most recent and the deepest, played a key role in the interpretation of the deep geoelectrical data obtained in the study area. A reinterpretation of the TRA_45 well, based on the lithological features reported in the P1000, is shown in Figure S3.
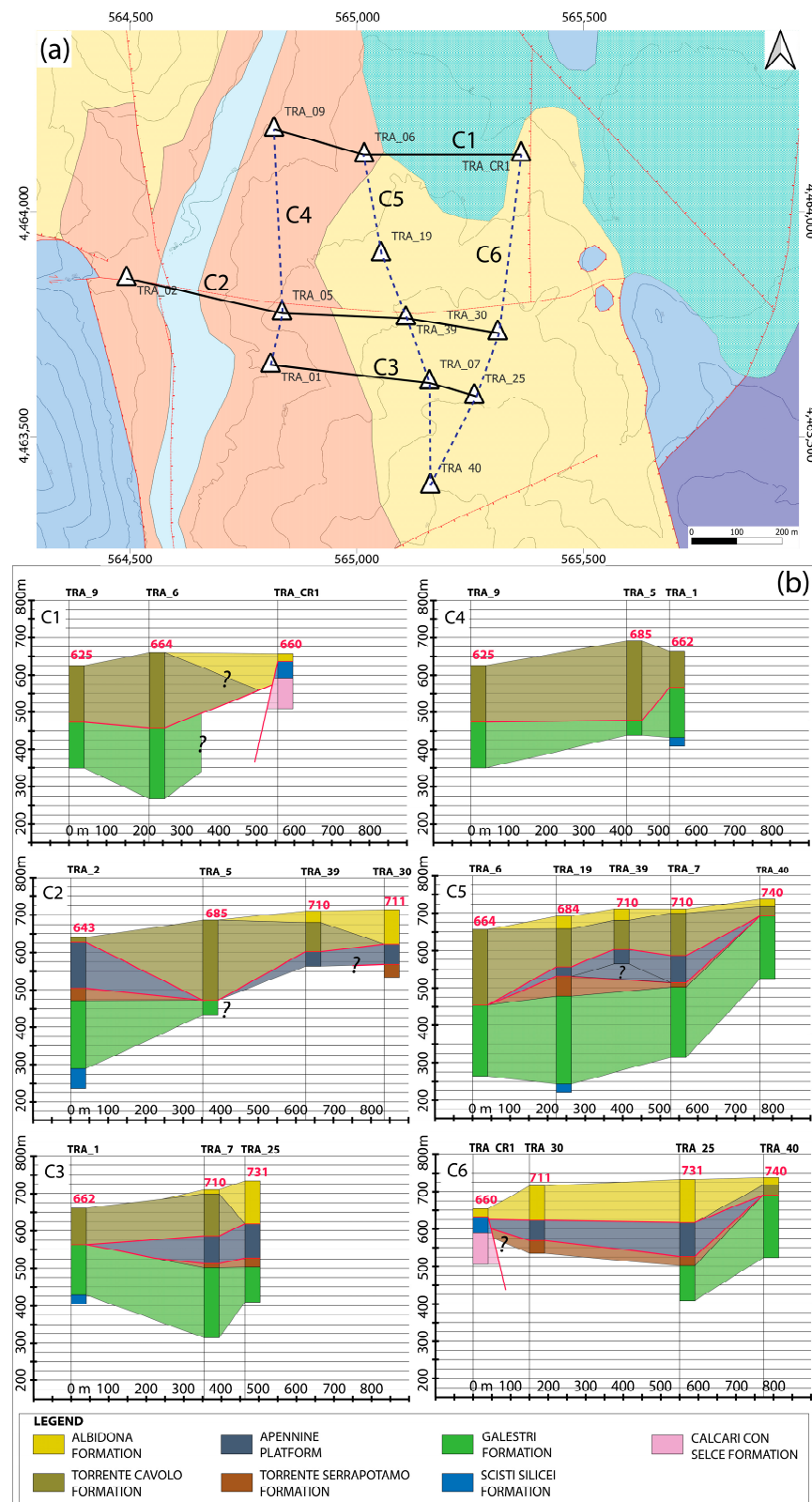
Figure 7. (**a**) Locations of some wells drilled in the study area. The wells present in the map were used for stratigraphic correlations (**b**). The C1, 2 and 3 correlation traces have been drawn with black lines in the E–W direction, while the C4, 5 and 6 traces are draw with dotted blue traces and are oriented in the N–S direction.

From the interpretation of the wells, the formations showed lateral thickness variations. From top to bottom, the stratigraphy included the Liguride Complex; the Apennine Platform Unit, not always present; and the Lagonegro II Unit. The Liguride Complex with the Albidona Formation had a maximum thickness of 61 m (TRA_32) considering the erosive contact on the surface, while the Torrente Cavolo Formation, where present, had thicknesses of up to 200 m (TRA_5) [88]. The Apennine Platform showed thicknesses ranging from 30 m to just over 90 m for the TRA_19 and TRA_2 wells, respectively. The formations of the Lagonegro Unit had varying thicknesses, according to the thrust with the overlying units; in fact, the Torrente Serrapotamo Formation, where present, had a maximum thickness of 50 m in the TRA_19 well, while the Galestri Formation in contact with the Scisti Silicei Formation, had thicknesses ranging from just over 130 m (TRA_1) to about 240 m (TRA_19). The Scisti Silicei Formation is 50 m thick in the TRA_CR1 well. It was overthrusted by the Albidona Formation at the top and and is in stratigraphic contact with Calcari con Selce at the bottom.

Figure 7 shows the correlations between the interpreted stratigraphic columns of the wells. Twelve wells, characterized with the most representative stratigraphies of the interpreted formations, were selected. The wells were correlated along traces with E–W (C1, C2 and C3) and N–S (C4, C5 and C6) orientations.

Well correlation allowed identification of tectonic contacts, such as high- and low-angle normal faults or thrusts, occurring between the tectonic units. In the case of the wells intercepting the limestone of the Apennine Platform Unit (Figures 7b and S1), the upper and lower limits were always interpreted as tectonic contacts. The correlation of the TRA_2 well log with the geological map (Figure 7) allowed interpretation of the upper tectonic contact of the Apennine Platform Unit as a low-angle normal fault. The prosecution of the same tectonic contact explains the complete elision of the Apennine Platform Unit in the TRA_ 9, 5 and 1 wells (Figure 7b; correlations C2 and C4), where the Liguride Complex rests directly on the Lagonegro Units. In the TRA_19, 39, 7, 30 and 25 wells (Figure 7b; correlations C5 and C6), a laterally discontinuous level of the Apennine Platform, characterized with thicknesses variations, was recognized. The Liguride Complex showed thickness variations and the nearly complete absence of the Torrente Cavolo Formation in the C6 correlation (detected only in the TRA_40 well). The correlation between the different Formations of the Lagonegro Units was hindered by the shallow depths investigated near the wells. It could be observed that the Torrente Serrapotamo Formation is absent in correlations C1 and C4: in the latter case, probably elided by a low-angle normal fault. The TRA_CR1 well showed the elisions of the Torrente Cavolo, Torrente Serrapotamo and Galestri Formations and the occurrences of the Scisti Silicei and Calcari con Selce Formations below the Albidona Formation. The contact between the Albidona and Scisti Silicei Formations was interpreted as being due to the presence of an N-striking normal fault intercepted by the well (Figure 7; correlation C1).

4.2.2. Geoelectrical Model of the Studied Area

In the DERT surveys, due to the large distance between the dipoles, the measured voltage signals were generally very low (<100 mV) and depended on the intensity of the injected current, the electrical characteristics of the medium and the interelectrode distances. Therefore, the acquired data underwent a series of analyses and processing.

For the Tramutola area, the first step consisted of current and voltage dataset synchronization; then, the voltage signals were processed by spike removal and signal detrending. Finally, FFT analysis was used to convert the voltage signal from its original time domain to a representation in the frequency domain. In particular, the amplitudes of the voltage signals in the frequency domain defined the electrical potential values at the current transmission frequencies (Figure 8). Subsequently, the apparent resistivity value (ρ_a) for each acquired ABMN quadrupole was estimated using Equation (1), with ρ_a values ranging from about 3 to 750 Ωm.
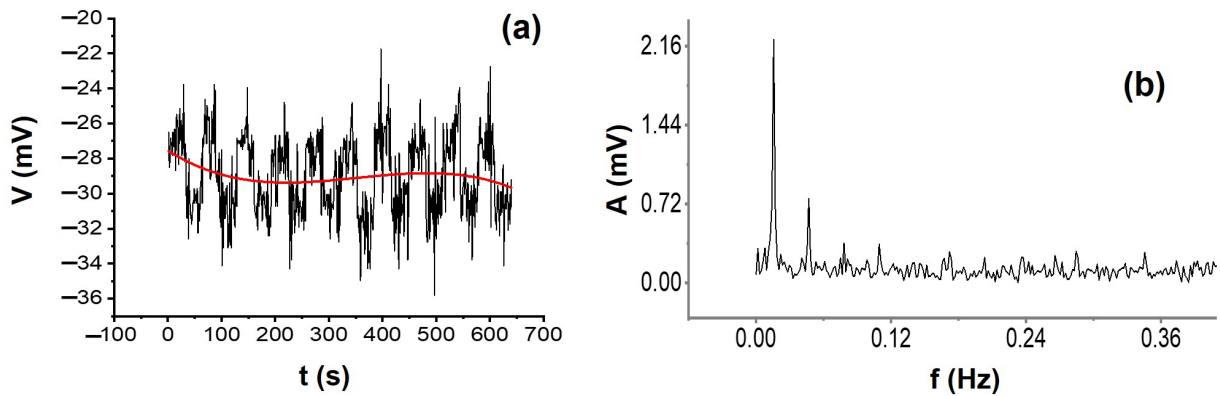
Figure 8. (**a**) Example of an electrical-potential-measured signal at the studied area. The red line represents a data polynomial trend. (**b**) Detrended electrical potential data in the frequency domain.

In order to reconstruct the real distribution of electrical resistivity in the subsurface, the ρ_a data were inverted using ZondRes2D software (from Zond Software Ltd., Pafos, Cyprus). Prior to the inversion process, a further data-processing phase was carried out consisting of graphing the measured electrical-resistivity data and defining filters to eliminate outliers and smooth out noisy areas. At the end of these analyses, approximately 25% of the data were excluded. Subsequently, once the topographical positions of all electrodes were indicated, 146 ρ_a data were inverted.

ZondRes2D software has the option of defining a rectangular mesh, of both the foreground and the background, that best subtends the profile so as to obtain all the cells where a resistivity model will be calculated according to the inversion algorithm used. In our case, a smoothness constraint, which is a least-squares inversion using a smoothing operator, was used. This algorithm results in a smooth (without sharp boundaries) and stable parameter distribution. Successively, Marquardt's algorithm was used; it is a classic inversion algorithm based on the least-squares method with damping-parameter regularization that allows better inversion of data via highlighting contrasting surfaces of electrical resistivity [93].

Figure 9 shows the inversion of the acquired data along the profile of the DERT (RMS < 4%), oriented from left to right and from SSW to NNE, respectively, with a depth of investigation down to approximately 400 m below sea level (about 1000 m from the ground surface).
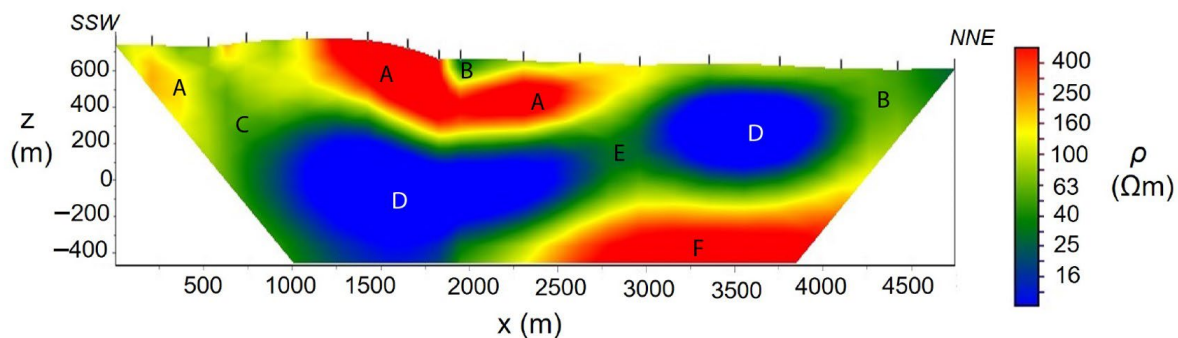

Figure 9. DERT results. The capital letters identify areas with different resistivities, whose values are shown in the resistivity bar (ρ in Ωm). A is the resistivity zones with $\rho > 120$ Ωm; B and C represent resistivity zones with $30 < \rho < 100$ Ωm; D have resistivity value < 30 Ωm; these low-resistivity bodies are separated with a higher-resistivity domain E with $\rho > 50$ Ωm; F has resistivity values $\rho > 150$ Ωm.

In detail, the DERT shows higher resistivity zones ($\rho > 120$ Ωm) at the surface in the southern corner and in the central portion of the tomography, this last having thickness decreasing toward the north (A). This resistive layer is surrounded with lower-resistivity zones ($30 < \rho < 100$ Ωm, B). Below, the DERT is characterized by lower electrical resistivity values (C). In particular, two low-resistivity domains ($\rho < 30$ Ωm), having sharp lateral boundaries, are present at the depths between 300 m a.s.l. and −400 m a.s.l. in the southern portion and between 550 and −250 m a.s.l. in the northern one (D). These low-resistivity bodies are separated with a higher-resistivity domain, with $\rho > 50$ Ωm (E). Finally, at the northern segment of the section, the base of the DERT profile shows a domain characterized with higher resistivity values ($\rho > 150$ Ωm, F).

5. Discussions
5.1. Synthesis of the Field and Subsurface Data

The Tramutola area is characterized with a complex structural setting that is difficult to understand unless approached holistically via integrating surface and borehole geological data and geophysical data. In detail, geology, fault geometry and kinematics were firstly determined with surface geological studies and analysis of well data. However, considering that most of the wells are quite shallow, geology and fault geometry at depths greater than 300 m are largely inaccessible. To improve on such limitations, a DERT survey was applied to establish detailed information at greater depth. The geological interpretation of the obtained resistivity model (Figure 10) reveals the detailed structural setting of the area down to an approximately 1000 m depth. This was obtained with the integration of surface geology (Figure 4) and the projection of TRA_2 and TRA_9 interpreted P1000s (Figure S3). Furthermore, additional information on the lithology and resistivity variations in the Lagonegro II Unit, coming from the deep TRA_45 well, has been considered. The TRA_45 resistivity log showed that the Galestri Formation is generally characterized with low resistivity values; on the contrary, electrical resistivity progressively increases in correspondence with the Scisti Silicei Formation. The Calcari con Selce Formation (from 200 to −375 m a.s.l.) generally shows internal resistivity variations linked to small changes in lithology, fracture intensity and bitumen presence. At the base of the Lagonegro II succession, the Monte Facito Formation is characterized with low resistivity values. Resistivity log values tended to increase again in correspondence with a tectonic repetition of the Lagonegro II succession, possibly connected to duplexing within this tectonic unit. At the well log bottom, at about −1700 m a.s.l., the Lagonegro II Unit overrode the Lagonegro I Unit. Finally, the following temperature values were recorded for the TRA_45 well: 28 °C at 194 m a.s.l. and 41 °C at the well bottom (−1225 a.s.l.).

As confirmed with the geological field work and the TRA_2 well log, A in Figures 9 and 10 corresponds to the Apennine Platform Unit (AP). Lower resistivity values at the surface (B) generally corresponded to the Torrente Cavolo (TCF) and Bifurto (BF) Formations in the southern sector and the Albidona (ALB) Formation in the northern sector. Down to about 470 m above sea level (a.s.l.), the interpreted logs reported the presence of the Lagonegro II Unit (Galestri, Scisti Silicei and Calcari con Selce Formations; C). Lower resistivity values in D were supposed, corresponding to more fractured LagonegroIIUnit rocks with water presence. Higher resistivity values in F were correlated to the tectonic repetition of the Lagonegro II succession. Finally, lateral and vertical resistivity contrasts showed a rather sharp transition throughout different resistivity domains in both the vertical (through means of subhorizontal contacts) and lateral (through means of subvertical contacts) directions. These last have been correlated with mapped high-angle faults. In particular, the higher resistivity domain, E, separating the low domains indicated with D, corresponds with the Fossatello right-lateral strike-slip fault.
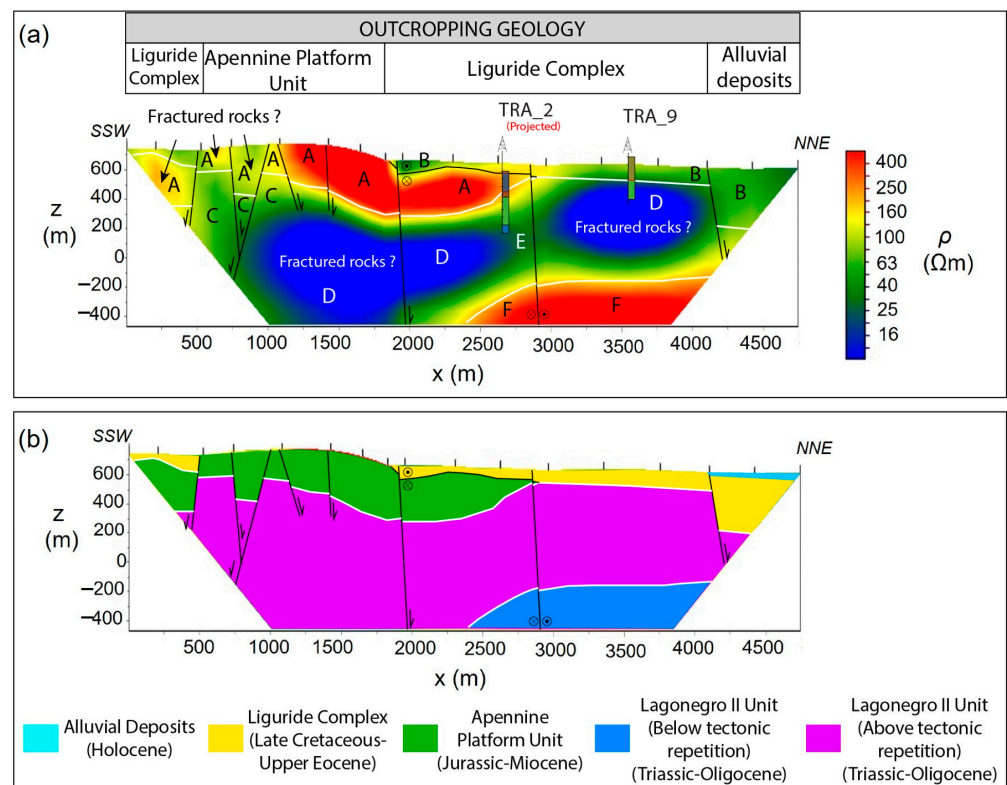
Figure 10. (**a**) Geological interpretation of the DERT results and comparison with outcropping geology. Black lines are high- and low-angle faults; white lines are thrusts. The kinematics are indicated with appropriate symbols. (**b**) Geological interpretation of the DERT, where units are shown with different colors.

Starting from the geological interpretation of the DERT in Figure 10, a 2D geological cross-section, intercepting the TRA_2, 9 and 45 wells, was constructed (a-a''' section, Figure 11). Moreover, the geometry of the tectonic structures in the study area was unraveled through means of three further 2D cross-sections, based on the surface data provided by the geological map (Figure 6) and the well data of the Tramutola field (Figure 7). In detail, the b-b' section, oriented NNW–SSE, intercepts the TRA_ 7, 9 and 19 wells; the c-c'' section, oriented NE–SW, intercepts the TRA_40 well; and the d-d'' section, oriented E–W, intercepts the TRA_2, 5 and 30 wells (Figure 11). These sections were further constrained by intersections with the a-a''' section.

The different orientations of the cross-sections allowed interpretation of the geometries of the various tectonic structures around the Tramutola oil field. The limestone of the AP Unit, outcropping at the eastern and western ends of section d-d'' (Figure 9), is generally characterized with thicknesses ranging from 50 to 200 m, as documented using the TRA_2 and 30 wells and field data. However, in the Macchia Michelina area, carbonate rocks decrease in thickness and disappear, as documented using the TRA_5 well. Very low thicknesses of carbonate rocks were documented in the b-b' section as well, with a maximum of about 70 m in the TRA_7 well and complete absence in the TRA_09 well. In section c-c'', the carbonate rocks reached a maximum thickness of about 300 m in the Fascitello–Rupe di Cavolo area. In this sector, platform limestones preserve SW-verging thrusts and duplex structures that were detected during field activity (Figure 6b). Finally, the nearly orthogonal section a-a''' allowed the interpretation of the thickness variations of the platform carbonates observed in sections b-b', c-c'' and d-d''. In particular, it could be observed that the Apennine Platform showed the maximum thickness in the southernmost sector, at the intersection with cross-section c-c''. There, carbonates are characterized with the shallow circulation of groundwater emerging at the Capocavolo springs. Toward the north, the tectonic contact separating the Liguride Complex from the platform carbonates is

a medium- to low-angle normal fault, N-dipping, exposed in the vicinity of the hydroelectric power plant (Figure 5). North of the TRA_2 well, platform carbonates thin gradually and disappear thanks to the presence of a low-angle normal fault.
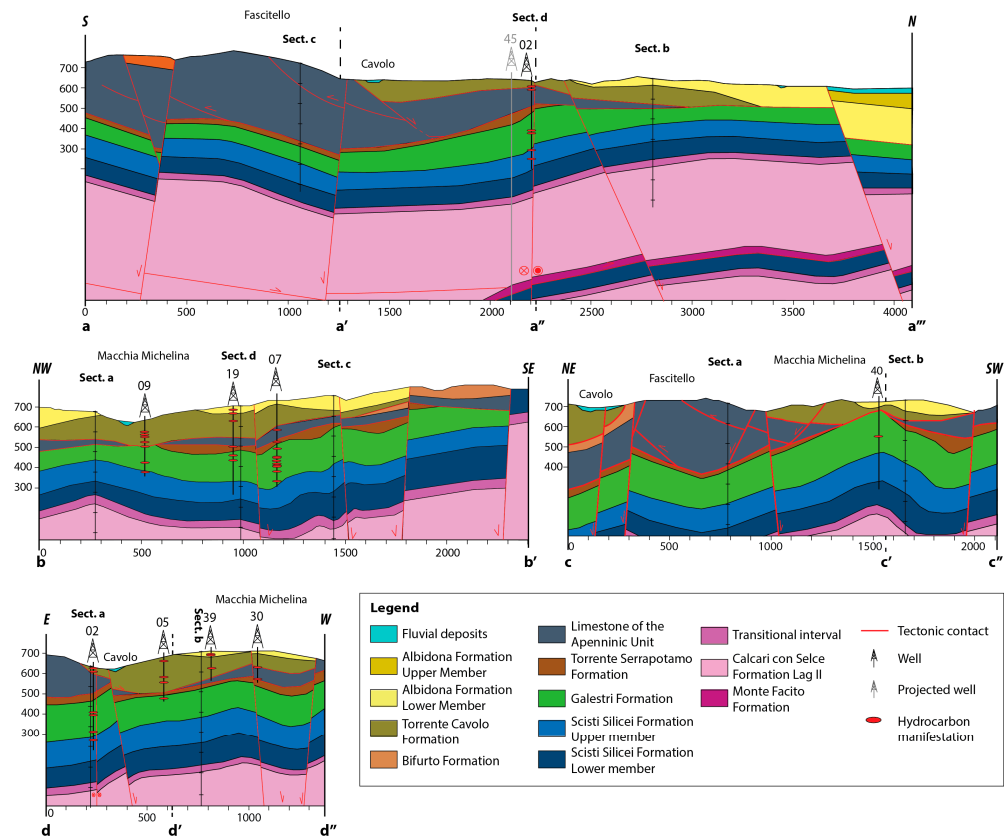

Figure 11. Geological cross-sections in the study area: section a-a‴, section b-b′, section c-c″ and section d-d″. The traces of the cross-sections are reported in Figure 5.

The Liguride Complex overlies the Apennine Platform and, locally, the Lagonegro Units along a low-angle tectonic contact that crosscuts the stratigraphic contact between the Cavolo and Albidona Formations. The Torrente Cavolo Formation shows a maximum thickness of up to 200 m along the right side of the Cavolo stream. The thickness of this Formation is strongly reduced up to being completely absent in the northeastern sector of the study area, where the Apennine Platform or the Lagonegro Units are directly covered with the Albidona Formation, which locally exceeds a thickness of 400 m in the northernmost sector of the study area. The tectonic contact between the Liguride Complex and the Lagonegro Units can be observed both in Macchia Michelina (Figure 11 Sect. B and D) and near the TRA_2 well. The Torrente Cavolo and Albidona Formations are characterized with intense deformation, with nearly E-trending, tight to open folds. This might explain the local thickness variations characterizing the Torrente Cavolo Formation.

The Lagonegro II Unit is exposed only in the southeastern sector of the study area. In particular, the presences of the Scisti Silicei Formation in the Bosco Armata area and of the Calcari con Selce Formation in the TRA_CR1 well log, north of the Macchia Michelina locality (Figure 7), allowed us to indicate a general uplift of the Lagonegro Units in the eastern sector of the study area. On the other hand, the area of the Tramutola oil field represents a tectonic depression, bounded by the Bosco Armata and Torrente Cavolo fault zones, where the Lagonegro Units are found at greater depths. For this reason, the tectonic structures affecting this unit were mainly deduced from the interpretation of the subsurface data. In particular, in Sections B, C and D (Figure 11), the Lagonegro II Unit appeared to be affected by upright anticlinal and synclinal folds, with wavelengths varying between

1 km and some hundreds of meters. The folds appeared truncated by the basal low-angle tectonic contact of the Apennine Platform above the Lagonegro Units. This interpretation is consistent with the large and frequent thickness variations of the Serrapotamo and Galestri Formations in the well logs and with the relative chronology between the thrusting of the Apennine Platform and the folding in the Lagonegro Units, recognized by previous authors [18,94]. The presence of N-trending folds in the Scisti Silicei Formation in the southeastern sector of the study area further constrains this interpretation.

5.2. The Structure of the Apennine Platform

The results of combining the DERT interpretation and the field geology allowed documentation of the intense brittle–ductile deformation affecting the tectonic units in this sector of the western High Agri Valley and particularly the Apennine Platform. This unit appeared significantly thinned with respect to the typical successions of the Agri Valley, where the thickness is about 700–800 m and may exceed 1 km in the Monti della Maddalena area [68]. As shown in the previous section, the maximum thickness of the Apennine Platform in the study area amounts to 300 m in a structural high located in the western sector of the geological map (Figure 5), between the Fossatello and Capo Cavolo localities. In this area, well-preserved contractional tectonic structures document SW-verging thrusting, implying tectonic thickening of the limestone, possibly connected to the emplacement of the Liguride Complex and the Apennine Platform above the Lagonegro Units during the Middle-to-Late Miocene period [60]. Eastward, in the area of the Tramutola oil field, the limestone of the Apennine Platform thins rapidly and mainly consists of a series of tectonic lenses, characterized with a thickness of a few tens of meters, aligned along the contact between the Liguride Complex and the Lagonegro Units. Thinning appears to be related to the presence of medium- to low-angle normal faults exposed along the western side of the Cavolo stream (Figure 5). Stretching connected to Late Pliocene low-angle normal faulting is responsible for exhumation of deeper tectonic units in the Southern Apennines [25] and is thought to be responsible for the tectonic thinning and boudinaging of the Apennine Platform in the study area.

Finally, different sets of high-angle normal faults affected the previous contractional and extensional tectonic structures. The main fault sets are NNW- to NW-trending normal faults, such as the Torrente Cavolo fault zone and other normal faults occurring in the Rupe del Cavolo and Capo Cavolo areas, and E-trending, dextral strike-slip faults. These faults are related to the Pleistocene to the present-day age extensional tectonic regime affecting the study area [28], and play a fundamental role in circulation of geofluids.

5.3. Inferences on Circulation of Deep Geofluids

With analysis of the subsurface data obtained with the DERT, it is suggested that the main resistivity contrasts are related to high- and low-angle tectonic contacts that influence shallow and deep fluid circulation (Figure 10a).

To the south, in correspondence with the Capo Cavolo springs, the Apennine Platform (AP) carbonates showed a lower resistivity response where the DERT crossed two NNW-trending faults (Figure 10). The electrical resistivity of carbonate rock–water systems is related to water content and rock porosity, especially crack connectivity [95]. Therefore, we suggest that the presence of the abovementioned faults affects both the fracture states and the water-saturation degrees of AP rocks, favoring water circulation in the shallower Monti della Maddalena groundwater systems.

At depth, rock bodies in the Lagonegro II Unit, with very low electrical resistivity, are assumed to be the reservoir of the hypothermal water flowing out of the TRA_2 well. In the southern part of the DERT, the conductive body shows a greater thickness. This has been interpreted as resulting from a greater thickness of the Calcari con Selce Formation, possibly connected to the presence of internal overthrusts.

As described in the TRA_45 well log, the Calcari con Selce Formation is characterized with internal variation in porosity, fracture intensity and, possibly, bitumen presence.

Probably, strata of well-bedded micritic limestone with high fracture intensity represent the main aquifer intercepted by TRA_2, while less fractured limestone and the clayey level of the Monte Facito Formation (from −400 m a.s.l. in the TRA_45 well log) may represent aquiclude. Furthermore, local higher resistivity values, both in the DERT results and in the TRA_45 resistivity log, could be associated with bitumen presence. The hypothesis that the Calcari con Selce Formation may represent a deeper aquifer was supported with both structural and hydrogeological studies. In detail, Mazzoli and Di Bucci [90], Mazzoli et al. [91] and Novellino et al. [92] underlined that brittle deformation results in increasing fracture permeability of the pelagic limestone of the Lagonegro Units. This is particularly effective in correspondence of fault intersections, where rock volumes are characterized with pervasive fracturing. Moreover, D'Ecclesiis and Polemio and [96] D'Ecclesiis et al. [97] described the presence of deep, high-pressure aquifers in the Calcari con Selce Formation in the Agri Valley.

The nearly vertical, more-resistive zone dividing the two conductive bodies under the TRA_2 well has been interpreted as a heavily deformed zone, possibly connected to the intersection between the Fossatello strike-slip fault with the medium- to low- angle fault and the Torrente Cavolo fault zone (Figure 5), where the uprising and migration of deep fluids, including hydrocarbon and gases, which generally have higher resistivity responses than does water, might be favored. Interestingly, several natural oil spills and gas upwellings [35] are located at the intersection between these faults.

6. Conclusions

This study focused on a very small area of the southern Apennines, extending for about 11 km^2 in the vicinity of the Tramutola village, where natural oil spills have been historically known since the 19th century and 48 wells, mostly unproductive, were drilled between 1937 and 1959. During research for hydrocarbons, hypothermal waters were discovered at a depth of about 400 m. Therefore, the studied area represents a key sector for exploitation of geothermal resources in abandoned oil fields and, possibly, for future reconversion of the productive oil wells located in the Agri valley into geothermal ones.

The study area is characterized with the presence of a complete section of the tectonic units that form the southern Apennines fold and thrust belt, which, from top to bottom, are the Liguride Complex, the Apennine Platform and the Lagonegro Units. In this work, geological and structural data acquired during a detailed field survey were compared with subsurface data from numerous well logs provided by Eni. Furthermore, a N–S deep electrical resistivity survey at the site was carried out. Through combining surface and subsurface data, a geological–structural map and four cross-sections to a depth of 400 m b.s.l. were constructed.

The main outcomes of this study are briefly outlined below.

- Field geology, reinterpretation of old wells and a deep ERT survey allowed interpretation of the geological setting of the study area down to a 1 km depth and reconstruction of the geometry of the tectonic structures.
- The western sector of the Agri Valley was affected by intense brittle–ductile deformation. In a first phase ductile and brittle deformation allowed the formation of contractional structures, followed by development of medium to low-angle faults derived by horizontal stretching.
- In a second phase (during the Quaternary), different sets of high-angle normal faults offset the previous structures.
- When placed in a wider context, the geological and structural data collected in the study area show that the carbonates of the Apennine Platform underwent significant tectonic thinning when compared with the typical successions exposed in the southern Apennines. Thinning was accomplished with the development of medium- to low-angle normal faults, which led to the boudinaging of the platform carbonates along the tectonic boundary between the Liguride Complex and the Lagonegro basin.

- The DERT obtained in the present study allowed reconstruction of the presence of deep aquifers bounded with shallow and steeply dipping tectonic contacts.
- The integration of surface and deep data suggested that the polyphase tectonic evolution recognized in the study area produced fault intersections that favored circulation and uprising of deep hypothermal fluids and, possibly, hydrocarbons.

Finally, to better assess the role played by the geometry of the tectonic structures in the circulation of deep geofluids, we are planning future research in this study area. In particular, we intend to acquire a second W–E-oriented DERT study. This will allow the construction of a 3D model in the study area.

References

1. Davídsdóttir, B. United nations sustainable development goals and geothermal development. In Proceedings of the SDG Short Course I on Sustainability and Environmental Management of Geothermal Resource Utilization and the Role of Geothermal in Combating Climate Change, Organized by UNU-GTP and LaGeo, Santa Tecla, El Salvador, 4–10 September 2016.
2. Soldo, E.; Alimonti, C.; Scrocca, D. Geothermal Repurposing of Depleted Oil and Gas Wells in Italy. *Proceedings* **2020**, *58*, 9. [CrossRef]
3. Watson, S.M.; Falcone, G.; Westaway, R. Repurposing Hydrocarbon Wells for Geothermal Use in the UK: The Onshore Fields with the Greatest Potential. *Energies* **2020**, *13*, 3541. [CrossRef]
4. Santos, L.; Dahi Taleghani, A.; Elsworth, D. Repurposing abandoned wells for geothermal energy: Current status and future prospects. *Renew. Energy* **2022**, *194*, 1288–1302. [CrossRef]
5. Molli, G.; Doveri, M.; Manzella, A.; Bonini, L.; Botti FMenichini, M.; Montanari, D.; Trumpy, E.; Ungari, A.; Vaselli, L. Surface-subsurface structural architecture and groundwater flow of the Equi Terme hydrothermal area, northern Tuscany Italy. *Ital. J. Geosci.* **2015**, *134*, 442–457. [CrossRef]
6. Wellmann, F.; Caumon, G. Chapter One—3-D Structural geological models: Concepts, methods, and uncertainties. In *Advances in Geophysics*; Schmelzbach, C., Ed.; Elsevier: Amsterdam, The Netherlands, 2018; Volume 59, pp. 1–121. [CrossRef]
7. Van Dijk, J.P.; Affinito, V.; Atena, R.; Caputi, A.; Cestari, A.; D'Elia, S.; Giancipoli, N.; Lanzellotti, M.; Lazzari, M.; Oriolo, N.; et al. Cento Anni di Ricerca Petrolifera. L'Alta Val d'Agri (Basilicata, Italia meridionale). In Proceedings of the 1° Congresso dell'Ordine dei Geologi di Basilicata, "Ricerca, Sviluppo ed Utilizzo delle Fonti Fossili: Il Ruolo del Geologo", Potenza, Italy, 30 November 2012; pp. 29–77.
8. Crema, C. Il petrolio nel territorio di Tramutola (Potenza). *Boll. Soc. Geol. It.* **1902**, *21*, 36–38.
9. Bonarelli, G. Possibilità petrolifere nel territorio di Tramutola in Basilicata. *G. Geol.* **1932**, *7*, 25–46.
10. Agip. Relazione sui Risultati delle Ricerche Petrolifere Eseguite dall'Agip nel Permesso di Tramutola (Potenza). 5p. 1940. Available online: https://www.videpi.com/videpi/cessati/relazione.asp?titolo=858&relazione=2227 (accessed on 10 January 2022).

11. Cazzini, F.F. The history of the upstream oil and gas industry in Italy. In *History of the European Oil and Gas Industry*; Craig, J., Gerali, F., MacAulay, F., Sorkhabi, R., Eds.; Geological Society Special Publications: London, UK, 2018; Volume 465, pp. 243–274.

12. Francalanei, G.P.; Visintin, V. *Ubicazione e Previsioni di un Sondaggio Profondo nel Permesso "Tramutola"*; AGIP Mineraria, Ufficio Geologico Regionale: Naples, Italy, 1958; p. 5.

13. Aronica, F. *Manifestazioni di Idrocarburi nell'Italia Meridionale*; Con Schede Descrittive; AGIP Mineraria, Ufficio Geologico Regionale: Naples, Italy, 1959; p. 11.

14. Mazzoli, S.; Corrado, S.; De Donatis, M.; Scrocca, D.; Butler, R.W.H.; Di Bucci, D.; Naso, G.; Nicolai, C.; Zucconi, V. Time and spacevariability of "thin-skinned" and "thick-skinned" thrust tectonics in the Apennines (Italy). *Atti Accad. Naz. Lincei. Rendiconti. Cl. Sci. Fis. Mat. Nat.* **2000**, *11*, 5–39.

15. Menardi Noguera, A.; Rea, G. Deep structure of the Campanian-Lucanian arc (southern Apennines). *Tectonophysics* **2000**, *324*, 239–265. [CrossRef]

16. Morandi, S.; Ceraglioli, E. Integrated interpretation of seismic and resistivity images across the Val d'Agri graben (Italy). *Ann. Geophys.* **2002**, *45*, 259–271. [CrossRef]

17. Dell'Aversana, P. Integration loop of 'global offset' seismic, continuous profiling magnetotelluric and gravity data. *First Break* **2003**, *21*, 32–41. [CrossRef]

18. Shiner, P.; Beccacini, A.; Mazzoli, S. Thin-skinned versus thick-skinned structural models for Apulian carbonate reservoirs: Constraints from the Val d'Agri Fields, S Apennines, Italy. *Mar. Pet. Geol.* **2004**, *21*, 805–827. [CrossRef]

19. Turrini, C.; Renninson, P. Structural Style from the Southern Apennines' Hydrocarbon Province—An Integrated View. In *Thrust Tectonics and Hydrocarbon Systems*; AAPG Memoir; McClay, K.R., Ed.; American Association of Petroleum Geologists: Tulsa, OK, USA, 2004; Volume 82, pp. 558–578.

20. Megna, A.; Candela, S.; Mazzoli, S.; Santini, S. An analytical model for the geotherm in the Basilicata oil fields area (southern Italy). *Ital. J. Geosci.* **2014**, *133*, 204–213. [CrossRef]

21. Balasco, M.; Giocoli, A.; Piscitelli, S.; Romano, G.; Siniscalchi, A.; Stabile, T.A.; Tripaldi, S. Magnetotelluric investigation in the High Agri Valley (southern Apennine, Italy). *Nat. Hazards Earth Syst. Sci.* **2015**, *15*, 843–852. [CrossRef]

22. Balasco, M.; Cavalcante, F.; Romano, G.; Serlenga, V.; Siniscalchi, A.; Stabile, T.A.; Lapenna, V. New insights into the High Agri Valley deep structure revealed by magnetotelluric imaging and seismic tomography (Southern Apennine, Italy). *Tectonophysics* **2021**, *808*, 228817. [CrossRef]

23. Nicolai, C.; Gambini, R. Structural architecture of the Adria Structural architecture of the Adria platform-and-basin system. *Boll. Soc. Geol. Ital.* **2007**, *7*, 21–37.

24. Casero, P. Structural setting of petroleum exploration plays in Italy. *Spec. Vol. Ital. Geol. Soc. IGC* **2004**, *32*, 189–199.

25. Mazzoli, S.; Ascione, A.; Buscher, J.T.; Pignalosa, A.; Valente, E.; Zattin, M. Low-angle normal faulting and focused exhumation associated with late Pliocene change in tectonic style in the southern Apennines (Italy). *Tectonics* **2014**, *33*, 1802–1818. [CrossRef]

26. Prosser, G.; Palladino, G.; Avagliano, D.; Coraggio, F.; Bolla, E.M.; Riva, M.; Catellani, D.E. Stratigraphic and Tectonic Setting of the Liguride Units Cropping Out along the Southeastern Side of the Agri Valley (Southern Apennines, Italy). *Geosciences* **2021**, *11*, 125. [CrossRef]

27. Candela, S.; Mazzoli, S.; Megna, A.; Santini, S. Finite element modelling of stress field perturbations and interseismic crustal deformation in the Val d'Agri region, southern Apennines, Italy. *Tectonophysics* **2015**, *657*, 245–259. [CrossRef]

28. Maschio, L.; Ferranti, L.; Burrato, P. Active extension in Val d'Agri area, Southern Apennines, Italy: Implications for the geometry of the seismogenic belt. *Geophys. J. Int.* **2005**, *162*, 591–609. [CrossRef]

29. Burrato, P.; Valensise, G. Rise and Fall of a Hypothesized Seismic Gap: Source Complexity in the Mw 7:0 16 December 1857 Southern Italy Earthquake. *Bull. Seismol. Soc. Am.* **2008**, *98*, 139–148. [CrossRef]

30. Valoroso, L.; Improta, L.; De Gori, P.; Chiarabba, C. Upper crustal structure, seismicity and pore pressure variations in an extensional seismic belt through 3D and 4D Vp and Vp/Vs models: The example of the Val d'Agri area (southern Italy). *J. Geophys. Res.* **2011**, *116*, B07303. [CrossRef]

31. Stabile, T.A.; Giocoli, A.; Lapenna, V.; Perrone, A.; Piscitelli, S.; Telesca, L. Evidence of Low-Magnitude Continued Reservoir-Induced Seismicity Associated with the Pertusillo Artificial Lake (Southern Italy). *Bull. Seismol. Soc. Am.* **2014**, *104*, 1820–1828. [CrossRef]

32. Improta, L.; Bagh, S.; De Gori, P.; Valoroso, L.; Pastori, M.; Piccinini, D.; Chiarabba, C.; Anselmi, M.; Buttinelli, M. Reservoir structure and wastewater-induced seismicity at the Val d'Agri oilfield (Italy) shown by three-dimensional Vp and Vp/Vs local earthquake tomography. *J. Geophys. Res. Solid Earth* **2017**, *122*, 9050–9082. [CrossRef]

33. Bello, S.; Lavecchia, G.; Andrenacci, C.; Ercoli, M.; Cirillo, D.; Carboni, F.; Barchi, M.R.; Brozzetti, F. Complex trans-ridge normal faults controlling large earthquakes. *Sci. Rep.* **2022**, *12*, 10676. [CrossRef] [PubMed]

34. Cello, G.; Invernizzi, C.; Mazzoli, S.; Tondi, E. Fault properties and fluid flow patterns from Quaternary faults in the Appennines, Italy. *Tectonophysics* **2001**, *336*, 63–78. [CrossRef]

35. Italiano, F.; Martelli, M.; Martinelli, G.; Nuccio, P.M.; Paternoster, M. Significance of earthquake-related anomalies in fluids of Val D'Agri (southern Italy). *Terra Nova* **2001**, *13*, 249–257. [CrossRef]

36. Colangelo, G.; Heinicke, J.; Lapenna, V.; Martinelli, G.; Mucciarelli, M. Investigating correlations of local seismicty with anomalous geoelectrical, hydrogeological and geochemical signals jointly recorded in Basilicata Region (Southern Italy). *Ann. Geophys.* **2007**, *50*, 527–538. [CrossRef]

37. Storz, H.; Storz, W.; Jacobs, F. Electrical resistivity tomography to investigate geological structures of the earth's upper crust. *Geophys. Prospect.* **2000**, *48*, 455–471. [CrossRef]

38. Suzuki, K.; Toda, S.; Kusunoki, K.; Fujimitsu, Y.; Mogi, T.; Jomori, A. Case studies of electrical and electromagnetic methods applied to mapping active faults beneath the thick quaternary. *Eng. Geol.* **2000**, *56*, 29–45. [CrossRef]

39. Tamburriello, G.; Balasco, M.; Rizzo, E.; Harabaglia, P.; Lapenna, V.; Siniscalchi, A. Deep electrical resistivity tomography and geothermal analysis of Bradano foredeep deposits in Venosa area (Southern Italy): Preliminary results. *Ann. Geophys.* **2008**, *203*, 2012. [CrossRef]

40. Balasco, M.; Galli, P.; Giocoli, A.; Gueguen, E.; Lapenna, V.; Perrone, A.; Piscitelli, S.; Rizzo, E.; Romano, G.; Siniscalchi, A.; et al. Deep geophysical electromagnetic section across the middle Aterno Valley (central Italy): Preliminary results after the April 6, 2009 L'Aquila earthquake. *Boll. Geofis. Teor. Appl.* **2011**, *52*, 443–455. [CrossRef]

41. Pucci, S.; Civico, R.; Villani, F.; Ricci, T.; Delcher, E.; Finizola, A.; Sapia, V.; De Martini, P.M.; Pantosti, D.; Barde-Cabusson, S.; et al. Deep electrical resistivity tomography along the tectonically active Middle Aterno Valley (2009 L'Aquila earthquake area, central Italy). *Geophys. J. Int.* **2016**, *207*, 967–982. [CrossRef]

42. Gresse, M.; Vandemeulebrouck, J.; Byrdina, S.; Chiodini, G.; Revil, A.; Johnson, T.C.; Ricci, T.; Vilardo, G.; Mangiacapra, A.; Lebourg, T.; et al. Three-dimensional electrical resistivity tomography of the Solfatara Crater (Italy): Implication for the multiphase flow structure of the shallow hydrothermal system. *J. Geophys. Res. Solid Earth* **2017**, *122*, 8749–8768. [CrossRef]

43. Carrier, A.; Fischanger, F.; Gance, J.; Cocchiararo, G.; Morelli, G.; Lupi, M. Deep electrical resistivity tomography for the prospection of low- to medium-enthalpy geothermal resources. *Geophys. J. Int.* **2019**, *219*, 2056–2072. [CrossRef]

44. Rizzo, E.; Giampaolo, V.; Capozzoli, L.; Grimaldi, S. Deep electrical resistivity tomography for the hydrogeological setting of Muro Lucano Mounts Aquifer (Basilicata, Southern Italy). *Geofluids* **2019**, *2019*, 6594983. [CrossRef]

45. Troiano, A.; Isaia, R.; Di Giuseppe, M.G.; Tramparulo, F.D.A.; Vitale, S. Deep Electrical Resistivity Tomography for a 3D picture of the most active sector of Campi Flegrei caldera. *Sci. Rep.* **2019**, *9*, 15124. [CrossRef]

46. Porras, D.; Carrasco, J.; Carrasco, P.; González, P.J. Imaging extensional fault systems using deep electrical resistivity tomography: A case study of the Baza fault, Betic Cordillera, Spain. *J. Appl. Geophys.* **2022**, *202*, 104673. [CrossRef]

47. Rizzo, E.; Giampaolo, V.; Capozzoli, L.; De Martino, G.; Romano, G.; Santilano, A.; Manzella, A. 3D deep geoelectrical exploration in the Larderello geothermal sites (Italy). *Phys. Earth Planet. Inter.* **2022**, *329–330*, 106906. [CrossRef]

48. Rizzo, E.; Colella, A.; Lapenna, V.; Piscitelli, S. High-resolution images of the fault-controlled High Agri Valley basin (Southern Italy) with deep and shallow electrical resistivity tomographies. *Phys. Chem. Earth* **2004**, *29*, 321–327. [CrossRef]

49. Rizzo, E.; Giampaolo, V. New deep electrical resistivity tomography in the High Agri Valley basin (Basilicata, Southern Italy). *Geomat. Nat. Hazards Risk* **2019**, *10*, 197–218. [CrossRef]

50. Improta, L.; Iannaccone, G.; Capuano, P.; Zollo, A.; Scandone, P. Inferences on the upper crustal structure of Southern Apennines (Italy) from seismic refraction investigations and sub-surface data. *Tectonophysics* **2000**, *317*, 273–297. [CrossRef]

51. Mazzoli, S.; Barkam, S.; Cello, G.; Gambini, R.; Mattioni, L.; Shiner, P.; Tondi, E. Reconstruction of continental margin architecture deformed by the contraction of the Lagonegro basin, Southern Apennines, Italy. *J. Geol. Soc.* **2001**, *158*, 309–319. [CrossRef]

52. Patacca, E.; Scandone, P. Geology of the Southern Apennines. *Boll. Soc. Geol. Ital.* **2007**, *7*, 75–119.

53. Patacca, E.; Scandone, P. Il contributo degli studi stratigrafici di superficie e sottosuolo alla conoscenza dell'Appennino Capano-Lucano. In Proceedings of the 1° Congresso dell'Ordine dei Geologi di Basilicata, "Ricerca, Sviluppo ed Utilizzo delle Fonti Fossili: Il Ruolo del Geologo", Potenza, Italy, 30 November–2 December 2012; pp. 97–153.

54. Malinverno, A.; Ryan, W.B. Extension in the Thyrrhenian sea and shortening in the Apennines as a results of arc migration driven by sinking of the lithosphere. *Tectonics* **1986**, *5*, 227–245. [CrossRef]

55. Gueguen, E.; Doglioni, C.; Fernandez, M. On the post-25 Ma geodynamic evolution of the western Mediterranean. *Tectonophysics* **1998**, *298*, 259–269. [CrossRef]

56. Rosenbaum, G.; Lister, G.S. Neogene and Quaternary rollback evolution of the Tyrrhenian Sea, the Apennines, and the Sicilian Maghrebides. *Tectonics* **2004**, *23*, TC1013. [CrossRef]

57. Mattei, M.; Cifelli, F.; D'Agostino, N. The evolution of the Calabrian Arc: Evidence from paleomagnetic and GPS observations. *Earth Planet. Sci. Lett.* **2007**, *263*, 259–274. [CrossRef]

58. Doglioni, C.; Harabaglia, G.; Martinelli, F.; Mongelli, F.; Zito, G. A geodynamic model of the Southern Apennines accretionary prism. *Terra Nova* **1996**, *8*, 540–547. [CrossRef]

59. Petrullo, A.V.; Agosta, F.; Prosser, G.; Rizzo, E. Cenozoic tectonic evolution of the northern Apulian carbonate platform (southern Italy). *Ital. J. Geosci.* **2017**, *136*, 296–311. [CrossRef]

60. Bucci, F.; Novellino, R.; Tavarnelli, E.; Prosser, G.; Guzzetti, G.; Cardinali, M.; Gueguen, E.; Guglielmi, P.; Adurno, I. Frontal collapse during thrust propagation in mountain belts: A case study in the Lucanian Apennines, Southern Italy. *J. Geol. Soc.* **2014**, *171*, 571–581. [CrossRef]

61. Giano, S.I.; Lapenna, V.; Piscitelli, S.; Schiattarella, M. Electrical imaging and self-potential surveys to study the geological setting of the Quaternary slope deposits in the Agri high valley (Southern Italy). *Ann. Geofis.* **2000**, *43*, 409–419.

62. Piedilato, S.; Prosser, G. Thrust sequences and evolution of the external sector of a fold and thrust belt: An example from the Southern Apennines (Italy). *J. Geodyn.* **2005**, *39*, 386–402. [CrossRef]

63. Bonardi, G.; Amore, F.O.; Ciampo, G.; De Capoa, P.; Miconnet, P.; Perrone, V. Il complesso Liguride. Auct.: Stato delle conoscenze e problemi aperti sulla sua evoluzione pre-appenninica ed i suoi rapporti con l'Arco Calabro. *Mem. Soc. Geol. It.* **1988**, *41*, 17–35.

64. Scandone, P.; Sgrosso, I. Flysch con Inocerami nella valle del Cavolo presso Tramutola (Lucania). *Boll. Soc. Nat. Napoli* **1964**, *73*, 166–175.
65. Vezzani, L. Distribuzione, facies e stratigrafia della formazione del saraceno (Albiano-Daniano) nell'area compresa tra il mare Jonio ed il torrente Frido. *Geol. Romana* **1968**, *7*, 229–275.
66. Vezzani, L.; Festa, A.; Ghisetti, F.C. *Geology and Tectonic Evolution of the Central-Southern Apennines, Italy*; Geological Society of America: Boulder, CO, USA, 2010.
67. Baruffini, L.; Lottaroli, F.; Torricelli, S.; Lazzari, D. Stratigraphic revision of the Eocene Albidona Formation in the type locality (Calabria, southern Italy). *Riv. Ital. Paleontol. Stratigr.* **2000**, *106*, 73–98.
68. Scandone, P.; Bonardi, G. Synsedimentary tectonics controlling deposition of mesozoic and tertiary carbonatic sequences of areas surrounding Vallo di Diano. *Mem. Soc. Geol. It.* **1968**, *7*, 1–10.
69. D'Argenio, B.; Pescatore, T.; Scandone, P. Structural pattern of the Campania-Lucania Apennines. *Quad. Ric. Sci.* **1975**, *90*, 313–327.
70. D'Argenio, B.; Pescatore, T.; Scandone, P. Schema geologico dell'Appennino Meridionale (Campania e Lucania). Atti del Conv. Moderne vedute sulla geologia dell'Appennino. *Accad. Naz. Dei Lincei* **1973**, *182*, 49–72.
71. Palladino, G.; Parente, M.; Prosser, G.; Di Stasio, A. Tectonic control on the deposition of the Lower Miocene sediments of the Monti della Maddalena ridge (Southern Apennines): Synsedimentary extensional deformation in a foreland setting. *Boll. Soc. Geol. It.* **2008**, *127*, 317–335.
72. Scandone, P. Studi di geologia Lucana: Carta dei terreni della serie calcareo-silico marnosa e note illustrative. *Boll. Soc. Nat. Napoli* **1972**, *81*, 225–300.
73. *Carta Geologica d'Italia 1972, Foglio 199 Potenza, Poligrafica e Cartevalori, Ercolano (Napoli), Scale 1:100,000*; Servizio Geologico d'Italia: Florence, Italy, 1969.
74. Butler, R.W.H.; Mazzoli, S.; Corrado, S.; De Donatis, M.; Di Bucci, D.; Gambini, R.; Naso, G.; Nicolai, D.; Scrocca, D.; Shiner, P.; et al. Applying thick-skinned tectonic models to the Apennine thrust belt of Italy-Limitations and implications. In *Thrust Tectonics and Hydrocarbon Systems*; AAPG, Memoir; McClay, K.R., Ed.; American Association of Petroleum Geologists: Tulsa, OK, USA, 2004; Volume 82, pp. 647–667.
75. Mazzoli, S.; Aldega, L.; Corrado, S.; Invernizzi, C.; Zattin, M. Pliocene-quaternary thrusting, syn-orogenic extension and tectonic exhumation in the Southern Apennines (Italy): Insights from the Monte Alpi area. In *Styles of Continental Contraction: Geological Society of America Special Paper*; Mazzoli, S., Butler, R.W.H., Eds.; Geological Society of America: Boulder, CO, USA, 2006; Volume 414, pp. 55–77. [CrossRef]
76. Schiattarella, M. Quaternary tectonics of the Pollino Ridge, Calabria-Lucania boundary, southern Italy. *Geol. Soc. Spec. Publ.* **1998**, *135*, 341–354. [CrossRef]
77. Brozzetti, F. The Campania-Lucania Extensional Fault System, southern Italy: A suggestion for a uniform model of active extension in the Italian Apennines. *Tectonics* **2011**, *30*. [CrossRef]
78. Carbone, S.; Catalano, S.; Lentini, F.; Monaco, C. *Carta Geologica del Bacino del Fiume Agri. Scala 1:50,000*; Cartografia SELCA: Firenze, Italy, 1991.
79. Servizio Geologico d'Italia. Note Illustrative della Carta Geologica d'Italia Alla Scala 1:100,000, Fogli 199 e 210 "Potenza e Lauria". 1971. Available online: http://sgi.isprambiente.it/geologia100k/mostra_pdf.aspx?pdffile=210.pdf. (accessed on 10 January 2022).
80. Servizio Geologico d'Italia; ISPRA. Carta Geologica d'Italia Alla Scala 1:50,000, Foglio 506 "Sant'Arcangelo". 2005. Available online: https://www.isprambiente.gov.it/Media/carg/506_SANT_ARCANGELO/Foglio.html (accessed on 10 January 2022).
81. Servizio Geologico d'Italia; ISPRA. Carta Geologica d'Italia Alla Scala 1:50,000, Foglio 505 "Marsico Nuovo". 2012. Available online: https://www.isprambiente.gov.it/Media/carg/489_MARSICO_NUOVO/Foglio.html (accessed on 10 January 2022).
82. Servizio Geologico d'Italia, ISPRA. Carta Geologica d'Italia Alla Scala 1:50,000, Foglio 505 "Moliterno". 2014. Available online: https://www.isprambiente.gov.it/Media/carg/505_MOLITERNO/Foglio.html (accessed on 10 January 2022).
83. Bonarelli, G. Relazione Geologica. Parte II. "Programma di Ulteriori Studi e Ricerche". 1932. Available online: https://www.researchgate.net/publication/268130832_Cento_Anni_di_Ricerca_Petrolifera_l%27Alta_Val_d%27Agri_Basilicata_Italia_meridionale (accessed on 1 October 2022).
84. Balasco, M.; Lapenna, V.; Rizzo, E.; Telesca, L. Deep Electrical Resistivity Tomography for Geophysical Investigations: The State of the Art and Future Directions. *Geosciences* **2022**, *12*, 438. [CrossRef]
85. Chibueze Okpoli, C. Application of 2D Electrical Resistivity Tomography in Landfill Site: A Case Study of Iku, Ikare Akoko, Southwestern Nigeria. *J. Geol. Res.* **2013**, *2013*, 895160. [CrossRef]
86. Scandone, P.; Sgrosso, I. Sulla paleogeografia della Penisola Sorrentina dal Cretacico superiore al Miocene. *Boll. Soc. Natur. Napoli* **1965**, *74*, 159–177.
87. Dietrich, D.; Scandone, P. The position of the basic and ultrabasic rocks in the tectonic units of the Southern Apennines. *Atti Accad. Pontaniana Napoli* **1972**, *21*, 61–75.
88. Bonardi, G.; Ciampo, G.; Perrone, V. La formazione di Albidona nell' Appennino calabro-lucano: Ulteriori dati stratigrafici e relazioni con le unità esterne appenniniche. *Boll. Soc. Geol. Ital.* **1985**, *104*, 539–549.
89. Grimaldi, S.; Summa, G. Caratteri idrogeologici ed idrogeochimici del settore meridionale dei Monti della Maddalena (Appennino Meridionale). *G. Geol. Appl.* **2005**, *2*, 348–356. [CrossRef]

90. Mazzoli, S.; Di Bucci, D. Critical displacement for normal fault nucleation from en-échelon vein arrays in limestones: A case study from the southern Apennines (Italy). *J. Struct. Geol.* **2003**, *25*, 1011–1020. [CrossRef]

91. Mazzoli, S.; Invernizzi, C.; Marchegiani, L.; Mattioni, L.; Cello, G. *Brittle-Ductile Shear Zone Evolution and Fault Initiation in Limestones, Monte Cugnone (Lucania), Southern Apennines, Italy*; Special Publications; Geological Society: London, UK, 2004; Volume 224, pp. 353–373. [CrossRef]

92. Novellino, R.; Prosser, G.; Spiess, R.; Viti, C.; Agosta, F.; Tavarnelli, E.; Bucci, F. Dynamic weakening along incipient low-angle normal faults in pelagic limestones (Southern Apennines, Italy). *J. Geol. Soc.* **2015**, *172*, 283–286. [CrossRef]

93. Marquardt, D.W. An algorithm for least-squares estimation of nonlinear parameters. *J. Soc. Ind. Appl. Math.* **1963**, *11*, 431–441. [CrossRef]

94. Mazzoli, S. Structural analysis of the Mesozoic Lagonegro Units in SW Lucania (Southern Italian Apennines). *Studi Geol. Camerti* **1992**, *12*, 117–146.

95. Jouniaux, L.; Zamora, M.; Reuschlé, T. Electrical conductivity evolution of non-saturated carbonate rocks during deformation up to failure. *Geophys. J. Int.* **2006**, *167*, 1017–1026. [CrossRef]

96. D'Ecclesiis, G.; Polemio, M. Condizioni di emergenza di alcune tra le principali scaturigini della Basilicata. *Geol. Romana* **1994**, *30*, 105–112.

97. D'Ecclesiis, G.; Polemio, M.; Sdao, F. Le sorgenti dell'alta valle del F. Agri (Italia meridionale): Caratteri idrogeologici e idrochimici. *Acque Sotter.* **1998**, *59*, 9–16.